Effects of Macromolecular Crowding on Protein Folding

- *in-vitro* equilibrium and kinetic studies on selected model systems

Alexander Christiansen

Kemiska Institutionen

Umeå 2013-11-20

Responsible publisher under swedish law: the Dean of the Faculty of Science and Technology

ISBN: 978-91-7459-764-6
Elektronisk version tillgänglig på http://umu.diva-portal.org/
Tryck/Printed by: Service Center KBC
Umeå Sweden 2013

众鸟高飞去

孤云独去闲

相看两不厌

只有敬停山

—李白

The birds have vanished down the sky.
Now the last cloud drains away.
We sit together, the mountain and I,
Until only the mountain remains.
-Li Bai

(Translated by Xiaowei Song)

Table of Contents

Abstract

Protein folding is the process whereby an extended and unstructured polypeptide is converted into a compact folded structure that typically constitutes its functional form. The process has been characterized extensively *in-vitro* in dilute buffer solutions over the last few decades. However, *in-vivo,* it occurs inside living cells whose cytoplasm is filled with a plethora of different macromolecules that together occupy up to 40% of its total volume. This large number of macromolecules restricts the space available to each individual molecule, which has been termed macromolecular crowding. Macromolecular crowding generates excluded volume effects and also increases the importance of non-specific interactions between molecules. It should favor reactions that reduce the total volume occupied by all molecules within the cytoplasm, such as folding reactions. Theoretical models have predicted that the stability of proteins' folded states should be increased by macromolecular crowding due to unfavorable effects on the extended unfolded state. To understand protein folding and function in living systems, we need to have a defined quantitative link between *in-vitro* dilute conditions (under which most biophysical experiments are conducted) and *in-vivo* crowded conditions. It is therefore important to determine how macromolecular crowding modifies the biophysical properties of proteins.

The work underlying this thesis focused on how macromolecular crowding tunes proteins' equilibrium stability and kinetic folding processes. To mimic the crowded cellular environment, synthetic sugar-based polymers (dextrans of different sizes and Ficoll 70) were used as crowding agents (crowders) in controlled *in-vitro* experiments. In contrast to previous studies which often have focused on one protein and one crowder at a time, the goal here was to perform systematic analyses of the relationships between the size, shape and concentration of the crowders and the equilibrium and kinetic properties of structurally-different proteins. Three model proteins (cytochrome c, apoazurin and apoflavodoxin) were investigated under crowding by Ficoll 70 and dextrans of various sizes, using a range of spectroscopic techniques such as far-UV circular dichroism and intrinsic tryptophan fluorescence. Thermodynamic models were used to explain the experimental results.

It was discovered that the equilibrium stability of all three proteins increased in the presence of crowding agents in a crowder concentration-dependent manner. The stabilization effect was around 2-3 kJ/mol and was greater for the various Dextrans than for Ficoll 70 at the same mass concen-

tration but independent of dextran size (for dextrans ranging from 20 to 70 kDa). A theoretical crowding model was used to investigate the origins of this stabilization. In this model, Dextran and Ficoll were modeled as elongated rods and the protein was represented as a sphere, with the folded sphere representation being smaller than the unfolded sphere representation. Notably, this model was able to reproduce the observed stability changes while only accounting for steric interactions. This correlation showed that when using sugar-based crowding agents, excluded volume effects can be studied in isolation with no contributions from nonspecific interactions.

Time-resolved experiments using apoazurin and apoflavodoxin revealed an increase in the folding rate constants while the unfolding rates were unchanged by the presence of crowding agents. For apoflavodoxin and cytochrome c, the presence of crowding agents also altered the folding pathway such that it became more homogeneous (cytochrome c) and gave less misfolding (apoflavodoxin). These results showed that macromolecular crowding restricts the conformational space of the unfolded polypeptide chain, making its conformations more compact. This in turn eliminates access to certain folding/misfolding pathways.

The results of the kinetic and equilibrium measurements on three model proteins, together with available data from the literature, demonstrate that macromolecular crowding effects due to volume exclusion are on the order of a few kJ/mol. Considering the numerous concentration balances and cross-dependent reactions of the cellular machinery, small changes in energetics/kinetics of the magnitudes found here can have dramatic consequences for cellular fitness. In fact, local and transient changes in macromolecular crowding levels may be one way of tuning cellular biochemical processes without invoking gene expression.

List of Abbreviations

CD	Circular Dichroism
DLS	Dynamic Light Scattering
DSC	Differential Scanning Calorimetry
FCS	Fluorescence Correlation Spectroscopy
FRAP	Fluorescence Recovery after Photobleaching
FRET	Fluorescence Resonance Energy Transfer
GuHCl	Guanidine Hydrochloride
IR	Infrared Spectroscopy
MD	Molecular Dynamics
NMR	Nuclear Magnetic Resonance
PEG	Polyethylene glycol
PGK	Phosphoglycerate Kinase
PVP	Polyvinylpyrrolidone
R_g	Radius of Gyration
SANS	Small angle neutron Scattering
SAXS	Small angle x-ray Scattering
SOD	Superoxide Dismutase
SPT	Scaled Particle Theory
SPR	Single Particle Tracking

Enkel sammanfattning på svenska

Proteiner verkar i en trång miljö

Proteiner utgör en av biologins viktigaste molekyler. De fungerar som byggmaterial, strukturelement, transportmedel och katalysatorer inne i cellerna. Att undersöka proteiners egenskaper i detalj kan ge ökad förståelse för hur celler, och därmed levande organismer, fungerar. Proteiner tillverkas inne i cellerna i form av långa aminosyrakedjor. Dessa kedjor genomgår sedan en spontan process som kallas proteinveckning för att nå sin slutgiltiga kompakta och funktionella form. Det finns många sjukdomar, t.ex. Alzheimers och Parkisons, som beror på fel i veckningsprocesserna.

Proteiners veckningsprocesser brukar undersökas i laboratorieexperiment i utspädda vattenlösningar. I motsats till denna artificiella miljö är en levande cell fylld med en stor mängd olika molekyler som tillsammans tar upp 40 procent av den totala volymen. En viktig fråga är om proteiners egenskaper är desamma i den trånga cellmiljö som i en utspädd *in-vitro-lösning*? I den trånga cellmiljön uppkommer effekter såsom ospecifika växelverkningar mellan molekyler, ändrad viskositet och så kallade 'excluded volume'-effekter. Excluded volume-effekten är en sterisk effekt som beror på att två molekyler inte kan uppta samma plats samtidigt. Är det trångt i lösningen leder excluded volume-effekten till att molekylformer som upptar mindre plats prioriteras över sådana former som tar upp mycket plats. Eftersom uppveckade proteiner tar upp mer plats än de kompakta aktiva formerna bör veckade proteiner stabiliseras i cellmiljö. Steriska effekter av den trånga cellmiljön kan också påverka stabiliteten av protein-protein-komplex och enzymatisk aktivitet jämfört med in vitro. Olika teoretiska modeller har tagits fram som förutspår hur excluded volume-effekten kan påverka proteiners stabilitet.

I arbetet som ligger till grund för denna avhandling har effekterna av cellliknande miljö på proteiners stabilitet (jämvikt) och veckningsreaktioner (kinetik) undersökts med hjälp av spektroskopiska metoder. Tre modellproteiner har studerats: cytokrom c, apoazurin och apoflavodoxin. För att skapa en miljö som liknar situationen i en cell har långa socker-baserade polymerer (dextraner av olika storlekar och Ficoll 70) använts som 'crowding-agenter'. Dessa molekyler tar upp plats men växelverkar ej med de undersökta proteinerna.

Jämviktsmätningar för apoazurin och cytokrom c visade att dessa proteiner stabiliseras i närvaro av crowding-agenter och effekten på stabiliteten berodde på koncentrationen av crowding-agent och på polymerens form. Ökningen i proteinstabilitet är i storleksordningen 2-3 kJ/mol. Även om denna effekt kan anses liten, kan den ha betydelse i levande celler där små förändringar kan påverkar många olika jämvikter som beror av varandra. En teoretisk modell som bara tar hänsyn till steriska interaktioner och modellerar crowding-agenterna som långa stavar kan reproducera de experimentella resultaten.

Tidsupplösta experiment visade att veckningshastigheten för apoazurin och apoflavodxin blir snabbare i närvaro av en crowding-agent. Också här är ökningen större om den tillsatta mängden crowding-agent ökades. Cytokrom c och apoflavodoxin veckas i reaktioner som innefattar felveckade temporära strukturer. För dessa proteiner upptäcktes att i närvaro av crowding-agent ändrades veckningsvägen så att det blev mindre felveckning och mer homogena reaktioner än i vattenlösning.

Experimenten som presenteras i denna avhandling visar på ett systematiskt sätt hur några olika proteiners stabilitet och veckning påverkas av cellliknande miljö. Från resultaten kan slutsatsen dras att socker-baserade polymerer är bra redskap för isolerade studier av ‘excluded volume‘-effekter utan bidrag från ospecifika interaktioner mellan polymer och protein.

List of Publications

I) **Alexander Christiansen**, Qian Wang, Antonios Samiotakis, Margaret S. Cheung, and Pernilla Wittung-Stafshede. 2010. Factors Defining Effects of Macromolecular Crowding on Protein Stability: An in Vitro/in Silico Case Study Using Cytochrome c. *Biochemistry 49* (31), 6519-6530

II) **Alexander Christiansen**, Pernilla Wittung-Stafshede. 2013. Quantification of Excluded Volume Effects on the Folding Landscape of Pseudomonas aeruginosa Apoazurin In Vitro, *Biophysical Journal*, Volume 105, Issue 7, 1689-1699

III) Loren Stagg, **Alexander Christiansen**, and Pernilla Wittung-Stafshede. 2011. Macromolecular Crowding Tunes Folding Landscape of Parallel α/β Protein, Apoflavodoxin. *Journal of the American Chemical Society 133* (4), 646-648

IV) Eefei Chen, **Alexander Christiansen**, Qian Wang, Margaret S. Cheung, David S. Kliger, and Pernilla Wittung-Stafshede. 2012. Effects of Macromolecular Crowding on Burst Phase Kinetics of Cytochrome c Folding. *Biochemistry 51* (49), 9836-9845

Publications not covered in the thesis

V) **Alexander Christiansen**, Qian Wang, Margaret S. Cheung and Pernilla Wittung-Stafshede. 2013. Effects of macromolecular crowding agents on protein folding in vitro and in silico. *Biophysical Reviews* 5 (2), 137-145

VI) Qian Wang, **Alexander Christiansen**, Antonios Samiotakis, Pernilla Wittung-Stafshede, and Margaret S. Cheung. 2011. Comparison of chemical and thermal protein denaturation by combination of computational and experimental approaches. II. *Journal Chemical Physics* 135, 175102-1 – 175102-12

VII) Jörgen Ådén, Marcus Wallgren, Patrik Storm, Christoph F. Weise, **Alexander Christiansen**, Wolfgang P. Schröder, Christiane Funk, Magnus Wolf-Watz. 2011. Extraordinary μs–ms backbone dynamics in Arabidopsis thaliana peroxiredoxin Q. *Biochimica et Biophysica Acta (BBA) - Proteins and Proteomics*, Volume 1814, Issue 12, P1880-1890

VIII) **Alexander Christiansen**, Pernilla Wittung-Stafshede. 2013. Synthetic crowding agent causes excluded volume interactions exclusively in tracer protein solution. Submitted.

Alexander Christiansen's Contributions:

Paper I: designed, performed, and analyzed *in-vitro* experiments. Assisted in writing the manuscript.

Paper II: designed, performed, and analyzed all experiments. Wrote the manuscript together with the co-author.

Paper III: performed and analyzed kinetic and equilibrium data for some protein variants. Helped with the revision version of the manuscript.

Paper IV: designed, performed and analyzed the chemical equilibrium experiments. Assisted in writing the manuscript.

1. Introduction

A living cell such as that shown in Figure 1 can be regarded as a small factory in which proteins function as the workhorses. Their importance lies in their role as catalysts for chemical reactions, but they also act as structural elements in the cytoskeleton, and as a means of communication that enable the cell to interact with its surroundings via secreted proteins. Proteins are encoded by genes, which are transcribed into RNA that is then processed and finally translated into a polypeptide by ribosomes. Depending on the protein's purpose, it may undergo a phase of post-translational processing to establish its functional status. The protein will then be degraded at some point, and the process will start again. Because proteins play essential roles in cells and life processes in general, it is very important to understand their properties and behavior.[1]

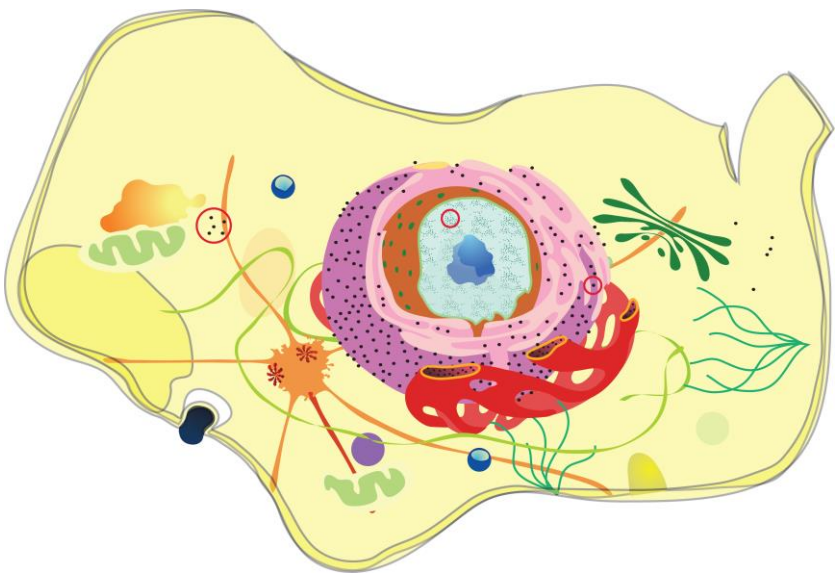

Figure 1) Cartoon of a eukaryotic cell showing the organelles and parts of the cytoskeleton.

This thesis is focused on protein folding due to its central role in protein biosynthesis. Folding is the process whereby an unstructured polypeptide chain is converted into a compact folded state. This often occurs via a cooperative two-state process, although the folding of longer polypeptide chains may involve one or more populated intermediates. The question is how a heteropolymeric chain of amino acids can obtain a distinctive three dimen-

sional structure. In particular, it is not clear why a polypeptide chain with a given sequence should usually adopt its final structure and in addition in most cases that process proceeds spontaneously without any help from other proteins, although larger protein might be dependent on chaperones as folding helpers.[2, 3] The information that determines which folded structure will be adopted and how it should be established must be somehow encoded in the polypeptide's amino acid sequence (and thus the sequence of the corresponding gene); deciphering this code is one of the Holy Grails of protein science.

1.1 Protein Folding

The structural information encoded within a protein's sequence can be investigated in both the folded and unfolded states. The folded state of a protein is often regarded as a single defined state, although folded proteins have a degree of flexibility that enables them to "breathe". The folded state is held together by hydrogen bonds and van der Waals-, ionic- (between charged groups) and hydrophobic interactions in the protein core. Covalent bonds are rare intracellularly and usually confined to disulfide bridges. The structure of a folded protein can be analyzed in hierarchical terms. Its primary structure is its amino acid sequence. The secondary structure consists of defined sub-structural elements such as α-helices and β-strands. The tertiary structure refers to the three-dimensional arrangement of the secondary structural elements. Finally, if the folded protein associates with other folded proteins to form a multimeric assembly (e.g. a homo- or hetero- dimer or trimer), it is said to exhibit a quaternary structure. Some proteins also incorporate non-protein cofactors such as metal ions that offer otherwise-unavailable functionality.[4] Information on the structure of folded proteins can be obtained using a plethora of techniques including Nuclear Magnetic Resonance (NMR)[5], cryo-EM[6] and X-ray crystallography (which can provide high resolution structures), as well as Circular dichroism (CD)[7], fluorescence[8], Raman[9] and infrared (IR)[10] spectroscopy.

The unfolded state is harder to characterize than the folded state. Instead of one defined structure, it is an ensemble of different chain conformations separated by small energy barriers, so interconversion between the different conformations proceeds readily.[11, 12] From his studies on chemically denatured proteins in 1972 Tanford concluded that the unfolded state probably adopts a random coil conformation.[13, 14] In general, no residual secondary structural elements or tertiary structure are apparent in the unfolded state, but exceptions have been reported.[11, 12, 15] Many experimental techniques that

can be applied to the folded state do not provide sufficient detail for analysis of the unfolded state. What can be measured *in-vitro* is the average extension of the unfolded state, using techniques such as small angle scattering (SAXS or SANS)[16], NMR[17, 18] or fluorescence resonance energy transfer (FRET)[19]. A SAXS study by Millett *et al.* compared results for a range of proteins of varying length in the folded and unfolded states using different means of denaturation. The authors proposed a power law relating the radius of gyration of the folded and unfolded states to the number of amino acids in the protein.[20] The scaling exponent for the unfolded state was found to be around 0.61. This is close to the value proposed by Flory (0.6) for the relationship between the extension of a real random coil polymer chain and the chain length.[21, 22] On the other hand, there are a range of proteins for which this relationship does not hold. These deviations could potentially be due to the retention of some residual structure in the unfolded state.[23, 24] FRET experiments have demonstrated that in some cases, the protein's radius of gyration increases with the concentration of denaturants such as urea or GuHCl.[25-27] However, no such increase was observed in SAXS studies conducted using the same solvent conditions.[28, 29] It is therefore possible that the observed dependence of the radius of gyration on the denaturant concentration is an artifact of the technique.[29]

The unfolded and folded states of a protein represent the start and end points of the protein folding reaction. Folding is a spontaneous process, so it decreases the free energy of the system. The free energy of folding for most proteins is relatively small (about ~20 kJ/mol).[30, 31] The overall free energy change of folding is determined by two large and opposing quantities: enthalpy and entropy.[30, 31] The ensemble of unfolded chain conformations is stabilized because it has many more degrees of freedom than the single folded state. In other words, the entropy of the unfolded ensemble is greater than that of the folded state. Conversely, the final folded state is enthalpically stabilized by hydrogen bonds in its secondary structure and hydrophobic interactions in the protein core. However, the loss in entropy and gain in enthalpy associated with the polypeptide chain alone are not sufficient to explain the whole process. The surrounding solvent (which is water for proteins *in-vivo*) must also be considered. There are two main factors that affect the entropy of water molecules during protein folding. First, in the unfolded chain, the hydrophobic side chains are exposed, so water molecules will be arranged around them in a highly immobile fashion. Additionally, polar groups and the hydrogen bond donors/acceptors of the amide backbone may form hydrogen bonds or other enthalpically favorable interactions with water molecules. The net effect results in an increase in entropy of water upon

folding, which partly compensates the loss in configurational chain entropy. Another enthalpic consequence of solvation is that unfolding changes the system's heat capacity by quite a large amount compared to the changes associated with reactions of smaller molecules. This is partly due to the large number of immobilized water molecules that surround the hydrophobic groups of the peptide chain. To recapitulate, proteins fold from an ensemble of unfolded states to a single compact folded state (Figure 2). The entropic and enthalpic changes that occur during folding as a result of within-chain and solvent-protein interactions produce a marginally stable folded state under physiological conditions.[30, 32]

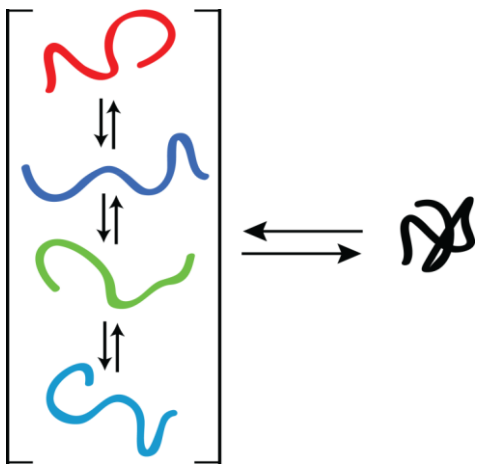

Figure 2) Cartoon showing a protein folding from different interconverting unfolded chain conformations to a single compact folded state.

What is the mechanism that enables a protein to find its final conformation over time? The number of pathways that could potentially lead from the unfolded-state ensemble to the final folded structure is enormous. This observation leads to the famous Levinthal paradox, which states that for a polymer chain to sample all possible conformations on its way to the final folded state would take more time than the age of the universe. [33] Because proteins can obviously transition from the unfolded to the folded state more quickly than this, they must have some sort of pre-sampling or path dependence, i.e. a bias towards certain conformations must exist. One possible explanation is embodied in the hydrophobic collapse model of folding in which higher order structural elements are formed around core interactions.[34, 35] A related hypothesis is the nucleation model, which suggests that a small core of secondary structure elements forms initially, which helps neighboring residues to adopt the correct structure.[36] A third model suggests that sec-

ondary structures form independently and the final step in the folding process involves their rearrangement to give the correct tertiary conformation.[37] All of these models resolve the Levinthal paradox by assuming that there is a bias towards a specific subset of the available conformations. However, it has yet to be determined which of these frameworks is correct, or whether there is one single framework that applies to all proteins.

In order to properly describe folding kinetics, there is one more state that must be probed: the high-energy transition state that connects the unfolded and folded states. Transition state theory was initially proposed by Eyring to describe the kinetics of reactions involving small molecules.[38] Its key concept is that there is a high energy barrier between the reactants and products. At that barrier a few key bonds are broken and formed, pushing the process in one direction. The application of transition state theory to the kinetics of protein folding is somewhat challenging because no covalent bonds are broken or made in the process; instead many weak interactions are broken and formed.[39] However, the assumption of a high energy barrier between the unfolded and folded states has been helpful in understanding and rationalizing folding processes. Structural information on folding transition states can be obtained indirectly through phi-value analysis, which was pioneered by Alan Fersht.[39, 40]

In summary, the equilibrium and kinetic properties of protein folding describe the transition from an ensemble of unfolded chain conformations to a single folded conformation. The process is complex and not fully understood at present. However, in order to understand how proteins attain their functional form *in-vivo*, there is another layer of complexity that must be considered: the cellular environment.

1.2 Macromolecular Crowding

1.2.1 Cell and Cellular Organization

The cell is the basic working unit of an organism; in the case of prokaryotes and single-celled eukaryotes, it is the entirety of the organism. In general, the cell is organized around its cytosol. In eukaryotic cells, the cytosol contains a set of membrane-encapsulated organelles such as the mitochondria and Golgi apparatus. Figure 1 shows a cartoon representation of an eukaryotic cell, with an outer cell membrane surrounding the cytosol and a set of distinct cellular compartments. However, this depiction fails to show the cytosol's complex composition. The cytosol contains all of the proteins, me-

tabolites, and machinery required for protein synthesis as well as the necessary raw materials. Figure 3 provides a more realistic representation of the cytosol. This figure clearly shows that due to its high content of macromolecules, there is actually not much 'free space' in the cytosol. The cytosol is therefore crowded. This crowdedness is not due to the presence of a single protein species (other than in certain cell types such as those of the eye lenses[41]), but to the total protein content. This phenomenon was termed "macromolecular crowding" by Minton in 1981.[42] The cellular compartments such as the mitochondria and nucleus are also filled with similarly crowded "cytosols".[43] The nucleus is a particularly interesting example because its cytosol can be further subdivided into nucleolar and chromosome domains.[44] While crowding occurs inside the organelles as well as the cytosol, the following discussion focuses on the cytosol for the sake of simplicity.

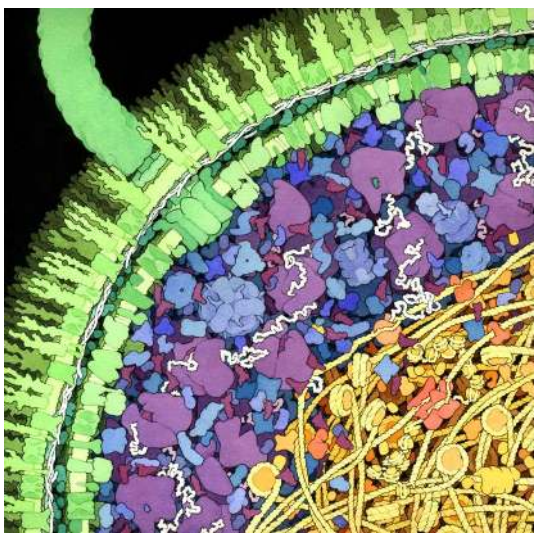

Figure 3) The cytoplasm of *E. coli* by Goodsell (1999). The cytoplasmic region is shown in blue and purple. The nucleotide region, which contains DNA wrapped around histones, is shown in yellow. Illustration by David S. Goodsell, the Scripps Research Institute; used with permission.

The number and type of molecules in the cytosol depend on the cell type and probably also on the cell cycle stage.[45, 46] The total quantity of protein in a cell is estimated to be around 50 -400 mg/ml, corresponding to 5-40% of its total volume.[47, 48] Zimmermann and Trach estimated the protein content of *E. coli* to be around 10 to 40% in units of weight/volume.[49] Similarly, Lanni *et al.* obtained a value of 200-300 mg/ml for 3T3 fibroblasts.[50] Since

most of the space in the cytosol is already occupied by other macromolecules, it is tempting to ask how proteins fold and function in such surroundings. This is particularly important because most of our current information on protein folding was obtained from *in-vitro* experiments in dilute solutions. In fact, experimentalists often strive to use the most dilute solution possible in order to avoid non-idealities and to focus on the "pure" protein properties. However, given the composition of the cytosol, non-idealities are to be expected. This raises another question: to what extent do inferences drawn from *in-vitro* experiments accurately represent the *in-vivo* situation? Various non-idealities could arise in the cytosol, such as excluded volume effects and non-specific interactions. In addition, the cytosol may be much more viscous than the very dilute solutions used for *in-vitro* studies.

Even this more "realistic" picture of the cytosol neglects an important layer of complexity: the spatial and temporal organization of the cytosol. The cytosol is not homogenous – its composition varies both spatially and temporally.[46, 51, 52] Differences in its local composition can cause density fluctuations and changes in the local concentrations of specific proteins. These differences can create what are effectively (micro-) compartments based on local density fluctuations rather than an enclosing membrane.[53]

1.2.2 Theoretical Models of Excluded Volume Effects on Proteins

The main aim of this thesis was to explore the consequences of excluded volume effects arising from steric repulsion. Excluded volume effects occur with all macromolecules and are particularly important *in-vivo* due to large number of macromolecules present in the cytosol. The concept of volume exclusion was first proposed by the polymer chemist Kuhn to explain the observation that real polymer chains tend to show less compaction than would expected in the absence of excluded volume effects.[54] The description of non-ideal gases (using the van't Hoff isobar) also relies on the concept of an excluded volume.[55] The simplest explanation of the phenomenon is that two molecules cannot occupy the same space at the same time. Consequently, there is a zone surrounding each molecule that cannot be entered by any other molecules without provoking a clash. This can be illustrated by considering a pair of solid spheres (Figure 4) whose centers must always be separated by at least the sum of their radii.

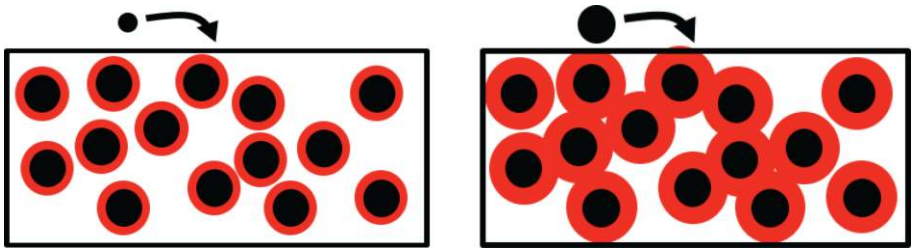

Figure 4) The excluded volume effect for the insertion of a sphere into a bath containing other spheres. The red areas in both figures indicate space that the new sphere cannot occupy without causing a clash. The left-hand figure shows the size of the excluded volume for the case where the diameter of the new sphere is half that of the background particles. The right-hand figure shows the case for a sphere of equal diameter.

The magnitude of the excluded volume effect between two molecules depends on their relative sizes and shapes. Non-spherical objects can have much larger exclusion volumes than spherical objects of the same volume.[42, 56] A theoretical modeling study examining real fluids was conducted by MacMillan & Mayer to investigate a related phenomenon.[57] They calculated the work required to place one new particle into a fluid containing a large number of other particles. Their solution relies on viral coefficients and a given interaction function between the molecules. An important restriction is that it uses only hard core repulsion, i.e. it assumes that the only effect of crowding is that the potential becomes infinite if the distance between two particles is less than the overlap distance. The advantage of this restriction is that the whole set of possible molecular interactions can be modeled by representing each particle as a single object with a defined shape and size. However, to address the general case, it is necessary to adapt this approach to systems with multiple types of molecules. The most common way of addressing this issue involves the use of approximate models based on scaled particle theory (SPT). This approach was initially developed to describe changes in activity for fluids consisting of hard spherical particles[58] but was later expanded to cover non-spherical particles as well.[59, 60] SPT is particularly useful for developing theoretical insights into the impact of macromolecular crowding on protein properties. Because proteins are polymers, the idea of volume exclusion can be extended to proteins in solutions containing large numbers of other proteins. One of the first theories of this type was developed by Laurent and Ogston in their study of size exclusion chromatography[61, 62], after Ogston's initial investigation into the effects of large concentrations of hyaluronic acid on protein partitioning.[63, 64] They assumed the

protein to be a sphere and the dextran chromatographic matrix to be an array of rods through which the proteins have to migrate. Minton subsequently built on these results to develop a model of protein activity using a hard-sphere approximation.[65] This approximation was based on the osmotic pressure dependence for concentrated solutions of hemoglobin, which were assumed to behave like collections of hard spheres that only interacted with one another via hard-core steric exclusion.[65-67] Minton later extended his model to describe protein folding/unfolding and protein association equilibria. In these models, he treated both the folded and unfolded states as approximate hard spheres, as shown in Figure 5.[68]

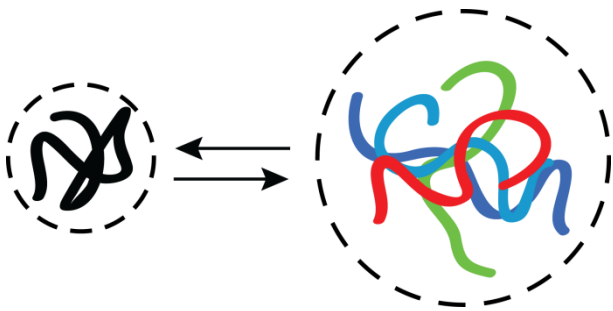

Figure 5) Hard particle representations of the folded and unfolded protein states. The left-hand side shows the hard sphere representation of the folded state, while the right-hand side shows that for the ensemble of unfolded polypeptide chains.

The average extension of all unfolded states is assumed to be greater than that of the compact folded state. Accordingly, the hard sphere representation of the unfolded state has a greater volume than the folded state. The effect of large, inert background molecules on protein folding equilibria was predicted by using Minton's hard sphere model with SPT.[56, 68] Folding in the presence of spherical background molecules was predicted to cause a non-linear increase in the equilibrium constant for folding. A similar model was later applied to non-spherical objects to estimate crowding effects on protein folding equilibria.[56] Other researchers also made predictions using approaches similar to Minton's but based on different assumptions for the unfolded state. For example, Zhou applied a Gaussian chain model for the unfolded state in the presence of spherical crowders, while keeping the hard sphere representation for the folded state.[69] Using this model, he predicted a change from stabilization to destabilization of the folded state at high crowd-

er concentrations because the Gaussian chain accommodates voids between the background molecules. This treatment led to a weaker destabilization of the unfolded state than the folded state. Minton subsequently proposed a similar model, assuming the unfolded state to behave like a Gaussian cloud. The extension of the unfolded ensemble was predicted to decrease, but there was no obvious change in the overall stabilization effect relative to that obtained using the earlier hard-sphere model.[70] All of these models are similar in that they treat the folded state as a hard sphere, but differ in their representation of the unfolded state.

The crowders are also typically modeled as hard particles (usually spheres) that only interact with the different protein states via hard-core repulsion. However, new approaches that incorporate attractive interactions between the crowder particles and proteins have recently been developed. Minton[71] and Zhou[72] assumed that the additional attractive interactions scaled with the exposed surface area, which implies that the unfolded state will experience more attractive interactions than the folded state. This assumption led to a stabilization of the unfolded state at sufficiently high crowder concentrations. It was further claimed that the additional attractive interactions had enthalpic effects whose magnitude should change with the temperature. When these contributions are considered, the net effect of crowding may be either stabilizing to destabilizing towards the folded state depending on the crowder concentration and temperature.

1.2.3 Experimental Studies of Macromolecular Crowding Effects

To test these theoretical predictions, it is necessary to create controlled crowded environments *in-vitro*. An ideal crowder should: 1) be highly soluble; 2) be similar in size to the target protein; 3) have a defined shape; 4) form no attractive interactions with the protein of interest; 5) not interfere with the spectroscopic techniques used to study the protein. Crowding with another protein may seem to be the most straightforward option since that would most closely represent the situation encountered in a cell. However, protein crowders usually are not soluble in high enough concentrations and also form numerous charge-charge interactions because proteins have charges distributed over their surface. It is therefore necessary to either screen these charges with either high salt concentrations or to just use low protein concentrations. Another important concern is that the spectroscopic techniques used to probe the target protein will be subject to interference from the protein crowder. Since the protein crowder is present at a much

higher concentration, it may dominate the signal and complicate the analysis. Last but not least, the background protein crowder should not undergo any folding/unfolding transition under the conditions used to induce folding in the protein of interest.

An alternative option is to use synthetic polymers, so called crowding agents, to induce the effects of macromolecular crowding. Polymers that have been used for this purpose include polyethylene glycol (PEG), Dextrans, Ficoll and Polyvinylpyrrolidone (PVP). PEG, PVP and Dextran offer the advantage that they can be prepared in different sizes. PEG is a polymer of ethylene glycol, PVP of N-vinylpyrrolidone, Dextran of glucose, and Ficoll of sucrose. They are all highly soluble (up to 400 mg/ml or more in water) and bear no charge at neutral pH. They do not have strong absorption above 210 nm nor are they fluorescent upon excitation at 280 nm. When studying excluded volume effects, it is desirable to avoid attractive interactions between the crowding agent and the protein of interest. There is evidence that PEG forms attractive interactions with proteins in addition to inducing volume exclusion.[73-75] PVP has not been used widely and the only group that had used it for protein stability studies found that it too forms unwanted attractive interactions with the protein.[76] Another important property of the crowding agents is their molecular shape. PEG and PVP are likely to be very flexible polymers.[77] In contrast, Ficoll has a more specific, spherical shape. This is because Ficoll is highly branched copolymer of sucrose and epichlorohydrin, which gives it a relatively compact and often sphere-like structure.[78-81] However, DLS studies have shown that Ficoll 70 adopts a shape that is intermediate between a sphere and a random coil.[82] In another study, Ficoll was modeled as a sphero-cylinder with a radius of 14 Å.[83] Dextran is a polymer of D-glucose with a lower degree of branching than Ficoll that adopts a more elongated, flexible shape.[81, 84, 85] Hydrodynamic radius values for different Dextrans have been determined by light scattering.[85]

Excluded volume effects on proteins due to macromolecular crowding had been investigated for some time, even before Minton coined the term in 1981. For example, it was demonstrated that the addition of PEG or Ficoll promotes the formation of HIV [86] and bacteriophage Φ29[87] capsids, which are large macromolecular assemblies. For individual proteins, the volume changes associated with folding or binding will be smaller than those for viral capsids, but are still predicted to be sufficiently large to give a macromolecular crowding effect. The following section discusses the effects of macromolecular crowding on phenomena such as association equilibria, enzymatic activity and the folding equilibria and structure of proteins.

In the case of association equilibria, there are two parameters that can potentially change during the reaction: the volume and shape of the monomer and multimer. Depending on how these parameters change upon association, steric repulsion may stabilize the associated state. The advantage of using association equilibria to study crowding is that they have well-defined start and end states. Snoussi and Halle reported a 30-fold increase in the association equilibrium constant for the formation of bovine trypsin inhibitor decamers based on NMR analyses.[88] Similarly, Diaz-Lopez *et al.* estimated a 10-fold increase in the equilibrium association constant for a RepA-DNA complex when using bovine serum albumin (BSA) as crowder.[89] In another study involving protein crowders (Ribonuclease A, RNase A and human serum albumin), Zorilla *et al.* used steady state and time-resolved fluorescence anisotropy to show that the self association of apomyoglobin increased in the presence of RNase A, but was unaffected by human serum albumin.[90] The free energy change for the conversion of human co-chaperonin 10 into a heptameric species increased by around 14 kJ/mol in response to crowding with 300 mg/ml Ficoll 70. It was further shown that this was primarily caused by effects on the stability of the individual monomers and that effects on the monomer-monomer interfaces were comparatively unimportant.[91] In 2010, Jiao *et al.* measured the binding of catalase to Superoxide dismutase (SOD) using Dextran and Ficoll 70 as crowders and found that the binding affinity increased by 3.6 kJ/mol in the presence of either crowder but concluded that the crowders' steric effects were tempered by attractive interactions.[92]

When analyzing enzymatic activity, it is important to understand how crowding affects the reaction mechanism and whether the reaction is diffusion- or transition state-controlled. Crowded solutions are more viscous than pure water. This will increase diffusion times, which will reduce the rate of diffusion-controlled reactions and so would reduce enzymatic activity rather than increasing it due to any change in volume.[93] Especially for reactions involving small substrates, the changes in volume on going from the free protein and substrate to the substrate-protein complex to the free protein and products can be very small. Indeed, Homchaudhuri *et al.* reported an increase in the catalytic rate for alkaline phosphatases in the presence of Dextran and Ficoll.[94] Moran-Zorzano *et al.* also found that high concentrations of PEG increased the rate of the reaction catalyzed by AspP from *E. coli*.[95] However, Derham and Harding observed a linear decrease in the activity of urease in the presence of increasing concentrations of Dextran or PEG, although the use of protein crowders caused a non-linear increase.[96] Similar non-linear crowding effects on enzymatic activity have also been

reported by Pozdnyakova and Wittung-Stafshede for multi-copper oxidase Fet3p. In this case, the addition of Ficoll or Dextran 20 initially increased the enzyme's K_m and K_{cat} values, which peaked at crowder concentrations of ~150 mg/ml.[97] The effects of crowding on enzyme kinetics have been reviewed by Vöpel and Makhadatzde, who reported that the addition of Ficoll 70 did not generally change the Michaelis constant or catalytic turnover number, but that some exceptions have been presented.[98] Overall, no common effect of macromolecular crowding on enzyme activity has yet been identified, and more studies in this area are needed.

Macromolecular crowding can also promote structural transformations. Most crowding theories predict a change in the relative free energies of the folded and unfolded states, assuming that the structures of the two states do not also change. The most obvious such change that might occur is that the expanded unfolded state may become compacted. Minton postulated a compaction of the unfolded state in the presence of crowding agents.[70] For adenylate kinase, Ittah *et al.* showed that adding Dextran 40 caused the distance between two residues in the unfolded chain to decrease but observed no such effect on the folded state.[99] Two other studies also reported similar unfolded state compaction in the presence of crowders based on two different techniques and two different proteins (CRAB I [100] and ribosomal protein S16 [101]). A more striking and unpredicted result was the finding that crowding by Dextran 70 or Ficoll 70 affected the folded structures of three proteins: apoflavodoxin, VlsE and phosphoglycerate kinase (PGK). Far-UV CD spectroscopic analyses indicated that crowding increased the secondary structure content of apoflavodoxin and VlsE in addition to affecting their equilibrium properties. These results were rationalized with the help of coarse-grained simulations [78, 102], and are important because they suggest that the folded structure observed *in-vitro* is not necessarily that adopted *in-vivo*. A subsequent *in-vivo* study by Dahr *et al.* provided some important support for this idea, showing that PGK also adopted a more compact tertiary structure *in-vivo* than had been observed *in-vitro*.[103]

Finally, a number of studies have reported crowding effects on protein folding equilibria and kinetics. There have been around 20 reports of crowding effects on thermal or chemical protein unfolding reactions based on studies using synthetic crowding agents. However, it is difficult to compare these studies directly because they generally used different types and concentrations of crowding agents. In most cases, the crowders increased the tested protein's equilibrium stability and resistance to thermal or chemical denaturation. However, the magnitude of the increased resistance to thermal

denaturation varied significantly from protein to protein. The midpoint of thermal denaturation increased by around 20 °C for the molten globular form of apomyoglobin in the presence of 270 mg/ml Dextran 30[104] while that of DNase I rose by around 15 °C in 200 mg/ml PEG[105]. Much more modest changes have also been reported: the midpoint for the thermal denaturation of PGK increased by only ~1.5 °C in 150 mg/ml Ficoll[103] while that of maltose binding protein increased by ~1.0 °C in the presence of 300 mg/ml Ficoll[106]. Compared to equilibrium studies, the effects of macromolecular crowding on protein folding kinetics have received relatively little attention. The refolding rate constant of carbonic anhydrase increased in the presence of Ficoll 70 but the total amount of refolded protein decreased.[107] Similarly, crowding caused reduced lysozyme to exhibit a slightly increased refolding speed but a reduced level of correct refolding due to aggregation.[108, 109] The refolding rate constants of VlsE[110], apoflavodoxin[79, 111] and apocytochrome b562[112] increased in the presence of crowders such as Ficoll, Dextran or PEG, but their unfolding rate constants were unaffected.

1.2.4 Computer Simulations of Crowding Effects

Computer simulations, especially molecular dynamics (MD) simulations have become important tools in crowding studies. It is difficult to calculate the excluded volume for non spherical objects, but simulations offer a way of approximating their effects. Such simulations can be simplified by using coarse-grained rather than all-atom approaches. In a coarse-grained simulation, individual amino acids (rather than individual atoms) are represented by balls and springs. This approach greatly reduces the number of interactions that have to be calculated. In both approaches, crowders are modeled as spheres or rods of a given size that only interact repulsively with the protein. Their sizes are often chosen to fit experimental data for Ficoll 70 and Dextrans. The simulations that have been reported correlate well with experimental findings and indicate that crowding destabilizes the unfolded state relative to the folded state.[113-118] A common finding in these studies was that crowding decreased the radius of gyration for the unfolded state.[118-120] A similar conclusion was drawn by Goldenberg, who performed a Monte Carlo simulation of a set of proteins and found that the unfolded state should be more compact.[121] MD simulations have shown that crowding accelerates peptide folding. Interestingly, however, the rate of folding does not increase linearly with crowder concentration; instead, it rises at low crowder concentrations and then starts to fall when the concentration is further increased.[117]

Elcock and Cheung both built models of the whole cytoplasm of the prokaryotic cell. Elcock's simulation showed that it was necessary to consider attractive interactions as well as excluded volume effects in order to explain the difference between computed results and *in-vivo* observations of the translational diffusion of green fluorescent protein.[122] Cheung *et al.* also showed that the melting temperature of a tracer protein (apoazurin) increased by 5 °C at equilibrium in a cytoplasm model.[123]

To sum up, computer simulations are a useful tool for predicting the effects of crowding on protein properties that can complement experimental data and provide key insights into the mechanisms by which various processes occur.

1.3 Aim of the Project

The cell is filled with macromolecules and so the intracellular environment differs from the dilute *in-vitro* conditions that are typically used in experimental studies on protein folding. Macromolecular crowding causes excluded volume effects, viscosity changes and changes in non-specific interactions. Theoretical models of volume exclusion predict that there should be differences between thermodynamic parameters measured *in-vitro* and those seen *in-vivo*. It is therefore important to experimentally characterize volume exclusion effects on protein biophysics. While many studies have addressed the stabilizing effects of macromolecular crowding on folded proteins, most of these studies have focused on only one crowding agent and one protein at a time.

The aim of the thesis is to use a range of "well behaved" model proteins to systematically investigate the effects of crowding agents with varying chemical properties and shapes, at different concentrations, on protein folding in terms of both equilibrium and kinetic effects. These effects were probed using equilibrium and time-resolved spectroscopy methods. The findings provide new insights into the underlying determinants of macromolecular crowding effects on protein folding and stability *in-vitro*, and show how these effects can be connected to *in-silico* simulations and theoretical models.

2. Materials and Methods

2.1 Protein Equilibrium Stability

The unfolding of a protein from a compact folded state to an ensemble of extended unfolded conformations can be described by the equilibrium constant for unfolding (K_U), which is defined as the ratio of the concentration of the unfolded (c_u) and the folded (c_f) states, or in normalized terms as the fraction unfolded (f_u) over the fraction folded (f_f). The corresponding free energy change of unfolding is ΔG_U and is related to K_U by the general gas constant (R) and the absolute temperature (T).

Reaction: Folded State Unfolded State

$$K_U = c_u/c_f = f_u/f_f \quad (1)$$

$$\Delta G_U = -R * T * \ln(K_U) \quad (2)$$

To obtain information about the equilibrium constant, the system must be disturbed using heat or chemical denaturants such as urea or GuHCl, with the latter being the stronger denaturant.[13] Important quantities in these modes of denaturation are the midpoints of chemical ($D_{1/2}$) and thermal denaturation (T_m), defined as the point at which K_U=1 or, in a two state process, where the fractions of folded and unfolded material are both equal to 0.5.

For chemical denaturation, the change in the free energy of unfolding can often be estimated by linear approximation.[124, 125] The observed changes in the transition region are then extrapolated to determine the value expected for a denaturant concentration of 0 M in order to estimate the protein's stability in buffer, $\Delta G_U(H_2O)$.

$$\Delta G_U(\text{GuHCl}) = \Delta G_U(H_2O) + m * [\text{GuHCl}] \quad (3)$$

Pace *et al.* found that the m-value (i.e. the derivative of equation (3) with respect to the GuHCl concentration) corresponds to the increase in solvent-accessible surface area upon denaturation. Accordingly, larger proteins will often exhibit higher m-value than smaller ones.[124, 126]

The free energy of unfolding for thermal denaturation can be determined as a function of the changes in enthalpy (ΔH_U) and entropy (ΔS_U) of unfolding according to

$$\Delta G_U = \Delta H_U - T * \Delta S_U \quad (4)$$

ΔH_U and ΔS_U are themselves temperature dependent.

$$\Delta S_U(T2) = \Delta S_U(T1) + \Delta c_p * \ln(T2/T1) \quad (5)$$

$$\Delta H_U(T2) = \Delta H_U(T1) + \Delta c_p(T2-T1) \quad (6)$$

Those expressions can be combined to yield (7), which gives the change in free energy on going from the starting temperature (T1) to the final temperature (T2).

$$\Delta G_U(T2) = \Delta H_U(T1) + \Delta c_p (T2-T1) - T2 * (\Delta S_U(T1) + \Delta c_p * \ln(T2/T1)) \quad (7)$$

Like the m-value, the change in heat capacity upon unfolding (Δc_p) partially reflects the protein's solvent-accessible surface area and therefore the difference in compactness between the folded and unfolded states. The m-value and Δc_p can therefore provide comparable information.[127] Δc_p can be determined by directly incorporating it into the fitting procedure as a free parameter. However, in many cases, the thermal data obtained from spectroscopy do not cover a wide enough range to allow reliable determination of Δc_p. DSC can enable the direct determination of Δc_p (usually with an error of about 10%), but can present other problems (see **2.5**).

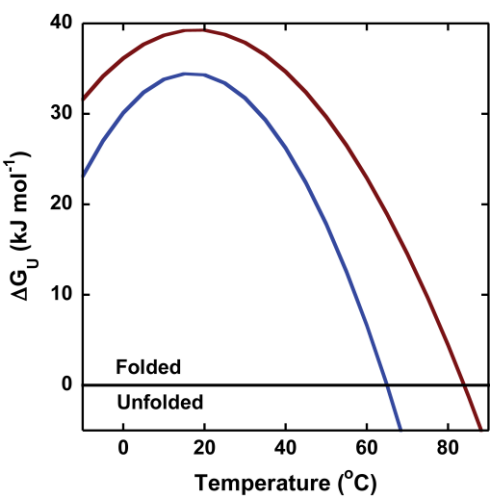

Figure 6) Change in the free energy of unfolding (ΔG_U) as a function of tem-

perature for two model proteins. Cytochrome c (red) has $\Delta H_U(T_m)$ = 410 kJ mol^{-1} with T_m = 84 °C and Δc_p = 5.6 kJ mol^{-1} K^{-1}. Apoazurin (blue) has $\Delta H_U(T_m)$ = 470 kJ mol^{-1} with T_m = 65 °C and Δc_p = 9.0 kJ mol^{-1} K^{-1}.

Since most of the acquired thermal data do not indicate large Tm shifts, Δcp is often assumed to be zero when extrapolating to a common temperature. The error in the ΔGU estimates obtained in this way was less than 0.3 kJ/mol. Figure 6 shows ΔGU as a function of temperature for two of the proteins used in this thesis.

2.2 Protein Folding Kinetics

The folding and unfolding of a protein via a two-state mechanism is a first-order process. It can be modelled using two differential equations that describe the change over time in the abundance of either the folded (F) or the unfolded species (U).

$$dF/dt = [U] * k_f - [F] * k_u \quad (8)$$

$$dU/dt = [F] * k_u - [U] * k_f \quad (9)$$

This is a system of two ordinary, linear differential equations with constant coefficients. Using the mass balance ([U] + [F] = [total]) and the initial conditions of F=0 at t=0, the solution to the system is

$$F(t) = F_{equ} - A * \exp(-t * (k_u + k_f)) \quad (10)$$

Here, F_{equ} is the equilibrium signal and the amplitude decay is A. The system can be disturbed using various measures such as heat[128], chemical denaturants or pressure[129]. Chemical denaturation is often performed in a stopped-flow instrument.[130] The contents of two syringes, one containing the protein in either a folded or unfolded state and one containing either buffer or denaturant, are quickly mixed. The resulting mixture enters a measurement cell, allowing the reaction to be followed as it moves towards the new equilibrium. Spectroscopic signals are probably the most common tools used to follow these changes. The resulting kinetic traces can then be fitted using a sum of exponentials to determine how many rate constants are needed to describe the process and their relative magnitude.

According to equation (10), the rate constants obtained from kinetic traces are equal to the sum of the forward and backward rate constants. When using chemical denaturants, the logarithm of the observed rate constants often

exhibit the same linear dependence as is seen for the free energy of unfolding in equilibrium. A plot of the logarithm of the observed rate constants for folding and refolding against the concentration of denaturant gives a v-shaped (Chevron) plot. The rate constants for unfolding and folding can then be obtained by extrapolating the refolding or unfolding limbs of this plot to a denaturant concentration of 0 M. Additional information can be obtained from the slopes of the two limbs.

$$\ln k_u = \ln k_u(H_2O) + m_u * [\text{denaturant}] \quad (11)$$

$$\ln k_f = \ln k_f(H_2O) + m_f * [\text{denaturant}] \quad (12)$$

The m-values of the folding (m_f) and unfolding (m_u) limbs of the Chevron plot can be used to calculate the Tanford β (T_β) value.[14, 131] This is a measure of the relative compaction of the transition state in the direction of the folded structure relative to the folded (T_β=1) and unfolded states (T_β=0).

$$T_\beta = m_f / (m_u - m_f) \quad (13)$$

Stopped-flow mixing can only be used to study reactions on timescales of milliseconds or longer. Its main limitation is the so-called dead time. The samples are mixed before the combined mixture enters the measurement chamber. Due to this delay, the starting point of a kinetic trace is not t=0. The dead-time of a stopped-flow instrument is around 2-4 ms, but it depends on the viscosity of the solutions used.

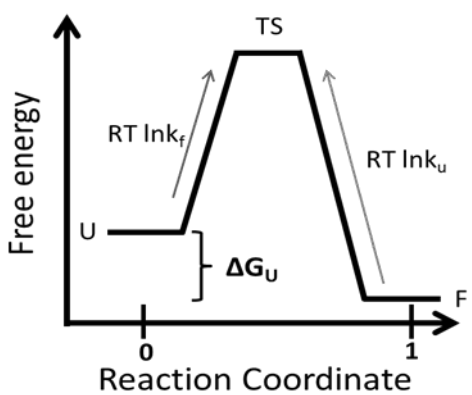

Figure 7) Free energy as a function of the reaction coordinate for a two-state process involving the unfolded (U), folded (F) and transition (TS) states, and the parameters that can be obtained from kinetic and equilibrium experi-

ments.

An advantage of kinetic over equilibrium measurements is the wider range of denaturant concentrations that can be studied. Equilibrium measurements are done at around the midpoint of denaturation, within a range of about 1 M or 10 °C, whereas the range of kinetic measurements extends almost all the way down to pure buffer for chemical denaturation.

2.2.1 Non-linearities and additional phases

Proteins (especially small ones[132]) can fold via a simple two-state process. Nevertheless, non-linearities are often observed in the limbs of Chevron plots, or multiple rate constants may be required to fit the kinetic traces.[132, 133] These are sometimes due to cis-trans proline isomerizations. The rate of these isomerizations can be around 0.1 s^{-1} – 0.01 s^{-1} and they are often separated from the main folding phase for fast folding proteins.[134-136] Various explanations have been proposed for cases involving roll-overs or curvature in the limbs of the Chevron plot, such as moving transition states[137, 138] and switches between different transition states.[139 140]

2.3 Comparing Kinetic and Equilibrium Measurements

The change in the free energy of protein unfolding (ΔG_U) can be measured using either equilibrium or kinetic methods (Figure 8). The equilibrium constant and kinetic parameters for a two-state process are connected via equation (14):

$$K_U = c_u/c_f = k_u/k_f \qquad (14)$$

This implies that both kinetic and equilibrium measurements should give the same result. Additionally the m-value for the equilibrium measurement (m_{equ}) should coincide with the sum of the individual kinetic m-values.

$$m_{equ} = (m_u - m_f) * RT \qquad (15)$$

A discrepancy between the kinetic and equilibrium values can point to a kinetic folding intermediate that is on or off pathway. One way of avoiding such intermediates is to restrict the analysis to a range surrounding the transition midpoint. Within this range, the limbs of the chevron plot are usually linear and provide information on the U-F transition.

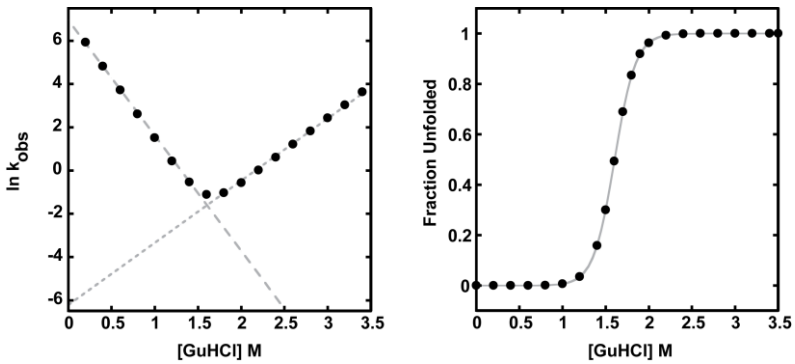

Figure 8) Examples of kinetic (left) and equilibrium (right) measurements for a simulated protein. The broken lines on the chevron plots show the refolding process. The kinetic parameters used were $k_f = 1042\ s^{-1}$ $k_u = 0.002\ s^{-1}$ $m_f = -13$ kJ, mol^{-1} $m_u = 7$ kJ mol^{-1} with a $\Delta G_U = 32$ kJ mol^{-1}, $D_{1/2} = 1.6$ M and $T_\beta = 0.65$. For the equilibrium curve, $m_{equ} = 20$ kJ mol^{-1} and $D_{1/2} = 1.6$ M were assumed, so $\Delta G_U = 32$ kJ mol^{-1}.

2.3.1 Phi-value analysis

The combination of protein folding kinetics and the introduction of point mutations makes it possible to obtain structural information on the otherwise unobservable transition state. The idea of phi value analysis is to introduce a point mutation, measure the equilibrium stability and folding kinetics for the mutant, and compare it to wild type data (Figure 9).[40] Assuming that the unfolded state remains unperturbed upon mutation, the ratio of the change in the free energies of the transition state ($\Delta\Delta G_{trans\text{-}F}$) and the folded state ($\Delta\Delta G_{U\text{-}F}$) due to the mutation gives the phi-value (Φ).

$$\Phi = \Delta\Delta G_{trans\text{-}F} / \Delta\Delta G_{U\text{-}F} \qquad (16)$$

The phi value indicates whether the mutated side chain forms native interactions in the transition state. A phi value of 1 would imply that the interaction of the mutated amino acid is important in the transition state; conversely, a value of 0 implies that the amino acid does not form important interactions in the transition state. Fractional phi values can be interpreted as evidence for a partial or weak interaction.[39] The choice of mutation is important to avoid introducing possible new interactions or increasing the flexibility of the amide backbone by adding a glycine residue. It is therefore common to use alanine as a substitute.[32] The magnitude of the change in $\Delta\Delta G_U$ is important and it has been pointed out by several authors that excessively small values can lead to unreliable phi values.[139, 141] Nevertheless, phi

value analysis has been successfully used for a range of proteins, giving information about the structures of their folding transition states.[142-145]

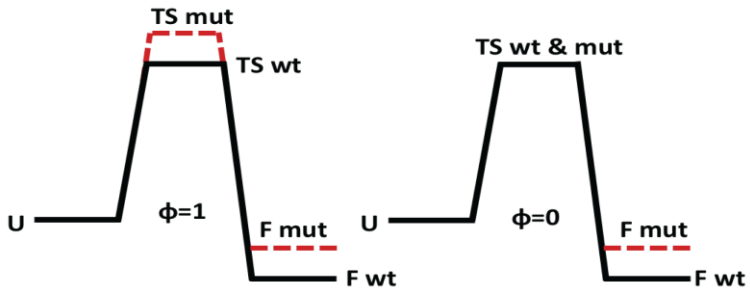

Figure 9) The concept of phi value analysis. Introducing a mutation (mut) changes the free energy of the folded state (F) but leaves the unfolded state (U) unperturbed. In the transition state, the destabilization due to the mutation is either fully present and results in a phi value of 1 (right) or absent, giving a phi value of 0 (left)

2.3 Spectroscopy

The changes in the equilibrium constant or kinetics in stopped-flow mixing can conveniently be measured using spectroscopic techniques. Amongst the more frequently used techniques are CD and fluorescence spectroscopy. Both are capable of giving structural information about the protein and are sensitive to changes in its conformation such as the change from a folded to an unfolded state. Its advantages include ease of use and the relatively low amount of protein required in typical experiments. The protein concentrations used in the experiments reported in this thesis were around 5 μM for fluorescence and 20 μM for CD experiments.

2.3.1 CD Spectroscopy

Circular dichroism describes the capacity of a molecule for differential absorption of left- and right-circularly polarized light. For proteins the main contribution in the far-UV region stems from the amide group in the protein backbone. The sensitivity of far-UV CD signals to the protein's secondary structure components (i.e. α-helices and β-strands) can be used to infer their relative abundance. The absorption maxima and line shape depend on the type of secondary structure and their relative abundance in the molecule. In principle, this makes it possible to determine the secondary structure composition of a protein by comparing a given CD spectrum against spectra of proteins with known secondary structures.[7]

In the case of protein unfolding, the difference in CD spectra between the folded and unfolded states can be used to determine ΔG_U. For a two-state system, it can be assumed that only folded and unfolded species exist in equilibrium and that the measured CD signal is a linear combination of the folded and unfolded signals. Thus, by measuring the CD spectra under different denaturing conditions, an unfolding curve can be obtained by plotting f_u against the concentration of GuHCl or the temperature.

2.3.2 Fluorescence Spectroscopy

Fluorescence is the light emitted by a molecule as it returns to its ground state after excitation. The three aromatic amino acids tryptophan, phenylalanine and tyrosine can be excited by light in the 260 -295 nm region. Since their excitation and emission spectra are dependent on their respective surroundings, they are good probes for investigating a protein's integrity. The probes sense their local environment and therefore provide localized information on protein structure. As in the case of CD spectroscopy, the difference between the emission spectra for the folded and unfolded states can be used to follow the denaturation of a protein by gradually changing the denaturing conditions. The advantage of fluorescence spectroscopy compared to CD is its greater sensitivity. This makes it possible to use lower protein concentrations, avoiding possible side reactions such as aggregation.[8]

2.4 Crowder Preparation

The Ficoll (Sigma-Aldrich) and Dextrans (Pharmacosmos, Denmark) powders used in the experimental studies readily dissolved in buffer without any heating. The concentrations of the crowder solutions were determined by measuring their optical rotation. The reducing sugar content of the Ficoll and Dextran solutions was determined to be around 0.1 % using 3,5-dinitrosalicylic acid, which was considered to be negligible.[146]

2.5 Differential scanning calorimetry (DSC)

DSC makes it possible to directly measure the heat released during protein unfolding, in contrast to the indirect inferences obtained using CD or fluorescence. DSC measures the energy needed to keep the temperature of a sample cell relative to a buffer cell constant while scanning through a temperature range. Processes that cause heat release or uptake (like protein unfolding) in the sample cell can thus be detected and quantified. Additionally, Δc_p can be obtained from the pre- and post-transitional baselines.

Because DSC only measures actual heat transfers, the thermograms are independent of the background protein concentration as long as the background species does not undergo any transitions. In principle, this means that it should be possible to measure the stability of one protein in the presence of a large background concentration of another protein, i.e. to investigate the effects of crowding one protein with another provided that their melting points are sufficiently far apart. Unfortunately, in a preliminary trial using ubiquitin and cytochrome c, it was found that the solubilities of the proteins were below 100 mg/ml. In addition, large shifts in the baselines for the crowding agents Ficoll and Dextran were observed during re-scans, probably due to oxidation. This made the estimated integrated ΔH_U values unreliable. The van't Hoff ΔH_U value that was obtained was comparable to that determined using CD and fluorescence, but the main advantage of DSC (i.e. the ability to directly measure heat exchange) was lost. In summary, while DSC could in principle be very useful for measuring the thermal stability of proteins, the stability problems encountered while using sugar crowders, the high required protein concentrations, and the inability to obtain results that cannot be obtained using CD or fluorescence spectroscopy precluded further experiments.

2.6 Model Proteins

The model systems chosen for the investigation of macromolecular crowding effects on protein folding were apoazurin, cytochrome c and apoflavodoxin. These proteins have been studied in dilute buffer systems and have been reported to fold via equilibrium two-state processes. Azurin and cytochrome c bind metal cofactors (copper and heme) while flavodoxin binds flavin mononucleotide (FMN). Table (1) summarizes some of the most interesting properties of the three proteins and figure 10 shows their structures. In the experiments, cytochrome c was used with the heme group attached but azurin and flavodoxin were used in their *apo* forms.

Table 1) General Parameters of the Model Proteins

Protein	Length	Fold	pI	Cofactor
Cytochrome c	104	α	9.6	heme
Flavodoxin	148	α/β	4.2	FMN
Azurin	128	β	5.7	Copper

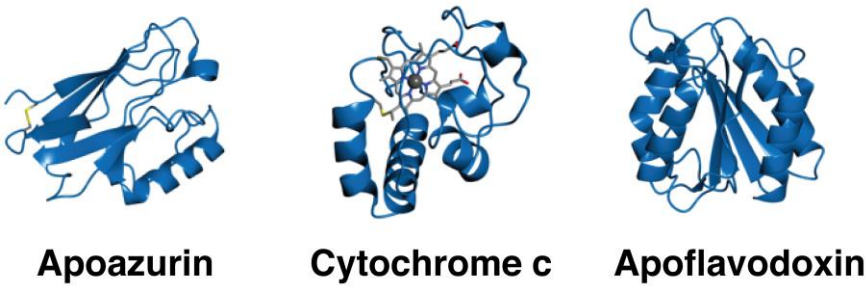

Figure 10) Three dimensional structures of the proteins used in the experimental studies, with their pdb codes in parentheses. Left, *Pseudomonas aeruginosa* apoazurin (3NP3) with the disulfide bridge between residues Cys3 and Cys26 in yellow. Middle, cytochrome c from *Equus caballus* (1HRC) with the heme group shown as a stick model and the complexed Fe^{3+} as a ball. Right, structure of *Desulfovibrio desulfricans* apoflavodoxin (3F6R).

2.6.1 Apoazurin

Azurin from *Pseudomonas aeruginosa* is a cupredoxin protein of 128 amino acids. It contains two β-sheets in a Greek-Key fold and it binds copper in a blue copper site.[147] The apo-form has been shown to unfold in a reversible two-state process under thermal and chemical denaturation.[148-151] Azurin was purified from *E. coli* using a periplasmic preparation with subsequent ion-exchange and gel-filtration. Bound zinc and copper were removed by potassium cyanide dialysis.[152] Azurin has a disulfide bridge between residues Cys3 and Cys26 that was not reduced in the experiments.

2.6.2 Cytochrome c

Cytochrome c is found in mitochondria and is associated to the outside of the inner membrane.[153] It is 104 amino acids in length with an α-helical structure and contains a prosthetic type C heme group that is attached to the polypeptide via cysteine residues 15 and 18. The coordinated iron is important for its function as an electron relay between complexes III and IV in the electron transport chain.[153, 154] Cytochrome c is well characterized in dilute buffer and has been reported to reversibly unfold under equilibrium conditions.[155-159] Oxidized (Fe^{3+}) cytochrome c is less stable towards chemical unfolding than the reduced form (Fe^{2+}). If oxidized cytochrome c is exposed to a GuHCl concentration that induces 100% unfolding, electron injection

leads to reduction and subsequent folding of the reduced form (Figure 11).[160-163] Cytochrome c from horse heart was bought as lyophilized powder (Sigma-Aldrich) and used without further purification.

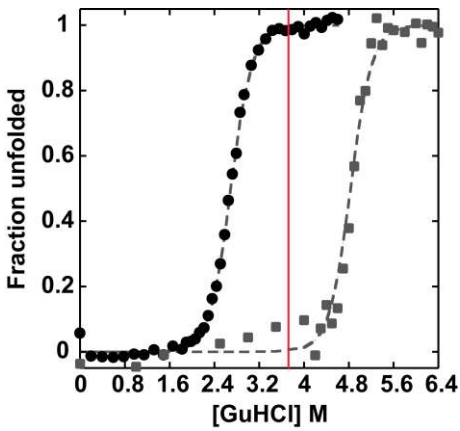

Figure 11) Chemical denaturation of oxidized (circles) and reduced (squares) cytochrome c showing the fraction unfolded as a function of the GuHCl concentration. The data for oxidized cytochrome c come from CD measurements at 220 nm while those for reduced cytochrome c are from heme absorption at 547 nm. The broken lines show two-state fits to the data. The vertical red line indicates the point at which laser-induced electron injection to the oxidized protein was used to trigger folding of the reduced form.

2.6.3 Apoflavodoxin

Flavodoxin from *Desulfovibrio desulfricans* is a 148 amino acid α/β protein that can bind to FMN as a redox active cofactor.[164-166] In previous studies, its thermal and chemical denaturation has been modelled as a two-state process, but the existence of an equilibrium folding intermediates has been postulated.[167, 168] Its folding kinetics have also been shown to involve off-pathway misfolding species.[164] The flavodoxin fold contains a central β-sheet consisting of five parallel β-strands surrounded by four α-helices (Figure 12). The source of early misfolding is an initial misalignment of the β-strands. Alignment at either end of the β-sheet results in misfolding. Correct folding can only proceed when the centre of the β-sheet is correctly aligned around β3.[169] Flavodoxin was purified from *E. coli*..[169] The apo and holo forms were separated on a cation exchanger and further purified by size exclusion chromatography. 13 point-mutated variants described earlier were used here for phi-value analysis.[169]

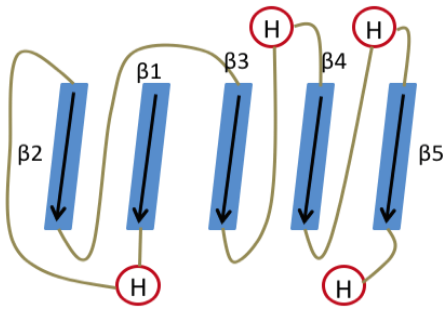

Figure 12) Schematic depiction of the flavodoxin fold. Four α-helices are arranged against a central β-sheet consisting of parallel β-strands 1 to 5.

2.7 Theoretical Models of Excluded Volume Effects on Protein Stability

In equation (1), the equilibrium constant was defined in terms of the concentrations of the involved species. The general definition involves the activity coefficients for the folded (γ_F) and unfolded (γ_U) state:

$$K_U = \gamma_U * c_U / \gamma_F * c_F \qquad (16)$$

In the ideal case, the activity coefficients equal one and equation (16) approaches equation (1). Expression (1) and (16) for the equilibrium constants are connected via expression (17), which links the composition-dependent apparent equilibrium constant of unfolding (K_U^{app}) with the ideal equilibrium constant (K_U).

$$K_U^{app} = c_U / c_F = \gamma_F / \gamma_U * K_U \qquad (17)$$

Deviations from ideality will change the activity coefficients for the folded and unfolded states. Steric exclusion due to macromolecular crowding is predicted to increase the activity coefficients of all involved species.[56] It follows from equation (17) that depending on the magnitude of the changes in the activity coefficients, the equilibrium will be changed in one direction or the other. Experimentally, the difference between the changes in free energy of unfolding (K_U^{app}) in the presence and absence of crowders is measured. Then, using equation (17), the change in the ratio of the activity coefficients can be calculated. To explain the changes in the activity coefficients, a molecular model is needed. A range of such models have been proposed to account for non-ideality assuming that hard core steric repulsion is the only force acting between the molecules in the system.

The model proposed by Minton used SPT and assumed the folded and unfolded states to be hard particles of a given size and geometry. It predicts how much work is needed to insert particles into a bath of other particles.[56, 68] The first model assumed the folded and unfolded state to be spherical, but subsequently the model was extended to non-spherical geometries (Figure 13, left).[56] For the insertion of a spherical particle into a bath of spherical background particles of uniform size, the change in the activity coefficient for the inserted particle is a function of the fractional volume occupation (ρ) and the ratio (z) of the radius of the inserted particle (r_p) to that of the crowding background particle (r_c).

$$-\ln\gamma = (3z+3z^2+z^3)\rho + (4.5z^2+3z^3)\rho^2+3z^*3\rho \quad (18)$$

$\rho = \Phi/(1-\Phi)$, where Φ is the volume fraction occupied by the crowder

This model predicts that the logarithm of the activity coefficient increases monotonically and nonlinearly with the concentration of the background species and the size of the inserted particle. The increase is larger for non-spherical particles because a sphere has the smallest surface area for a given volume, decreasing the probability of steric interaction.

The parameters needed in the general form of the model are the Kihara supporting function (H)[170] and the surface area (S) and volume (V) of the represented particles. The values for H, S and V for different geometries have been tabulated.[56]

The volume occupation by the crowder particles can be calculated using the number density (θ), the partial-specific volume (v_p^c) and the concentration (c, in mg/ml) of the crowder.

$$\Phi = \theta * v_p^c * c \quad (19)$$

Another approach for predicting volume exclusion effects on γ was taken by Ogston[63] and later by Minton.[68] As in the previous model, the folded and unfolded states were assumed to be hard spheres, but the crowders were modelled as long rods of a given thickness with a length that is much greater than the dimensions of the folded or unfolded states. Consequently, the length of the crowder does not affect the particle. The resulting equation for the model becomes:

$$-\ln\gamma = (1 + r_p/r_c)^2 * \rho \quad (20)$$

The determining parameters in this model are the radius of the folded and unfolded states and the thickness of the rods, along with the partial specific volume of the crowder. This model predicts a linear increase in the logarithm of the activity coefficient with the concentration of background species (rods) (Figure 13, middle).

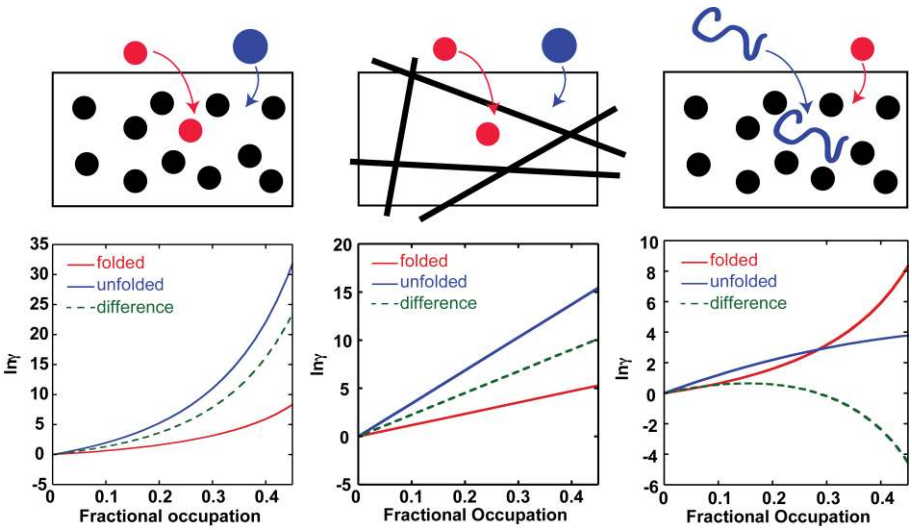

Figure 13) Predicted change in the activity coefficient as a function of fractional occupation by background molecules from the different crowding models for the insertion of a hard sphere of 1.7 nm (red) and 3.4 nm (blue) and the difference in the activity coefficients for the two particles (green). On the right, model 1 by Minton for the insertion into a solution containing hard spheres of 2.3 nm radius. Middle, Ogston model for insertion into a solution containing fibers of 7 Å diameter and "infinite" length. On the left, model by Zhou. The folded state is modeled according to model 1; the length of the chain in the unfolded state was assumed to be 104 residues. The background particles are hard spheres of 2.3 nm radius.

Another model proposed by Zhou[69, 171] treats the unfolded state as a Gaussian chain. Gaussian chains can be accommodated in voids between the solid sphere crowders. This is supposedly a more realistic treatment of the unfolded state and results in lower change in the activity coefficient of the unfolded state than the hard sphere representation. This treatment models the unfolded state according to:

$$-\ln\gamma_U = 3\Phi * y_m^2 + 6\pi^{-1/2} * \Phi * y_m^{1/2} - \ln(1-\Phi) - 9\Phi^2 * y_m^2 * \ln y_m \qquad (21)$$

where $y_m = R_s/6^{1/2} * r_c$ and the root mean square of the end-to-end distance R_s is a function of the length of the polypeptide chain (N), which was taken to be equal to[172]

$$R_s = 5.31 * N^{0.6} \quad (22)$$

The most interesting aspect of this model is the much weaker effect of the excluded volume on the unfolded state. For high crowder concentrations, this would result in a net destabilization of the folded state (Figure 13, right).

3. Results

The following section presents the main findings of the experimental studies included in this thesis. The majority of the data have been summarized in the publications that form the thesis' foundation, but some unpublished results are also presented. The experiments can be divided into equilibrium and kinetic measurements. The subsection **3.1** discusses the effects of Dextrans and Ficoll 70 on the equilibrium thermodynamic stability of cytochrome c and apoazurin; this is followed by a summary of the effect of macromolecular crowding on protein folding kinetics (section **3.2**).

3.1 Effect of Crowding on Equilibrium

The far-UV CD spectral data on the secondary structures of the studied proteins did not change following the addition of either Ficoll 70 or Dextrans of any size or at any concentration (Figure 14). This was true for both the folded and the thermally or chemically unfolded states. The same conclusion was drawn from the fluorescence emission spectra of the tryptophan environment. Visible CD can provide additional information on the integrity of the folded state of cytochrome c. The CD signal reporting on the heme-group at 409 nm did not change in the presence of crowding agents. Thus, at this level of resolution, the crowding agents did not affect the secondary structure content of any of the target proteins or the environments of the tryptophan or heme-group in apoazurin and cytochrome c, respectively.

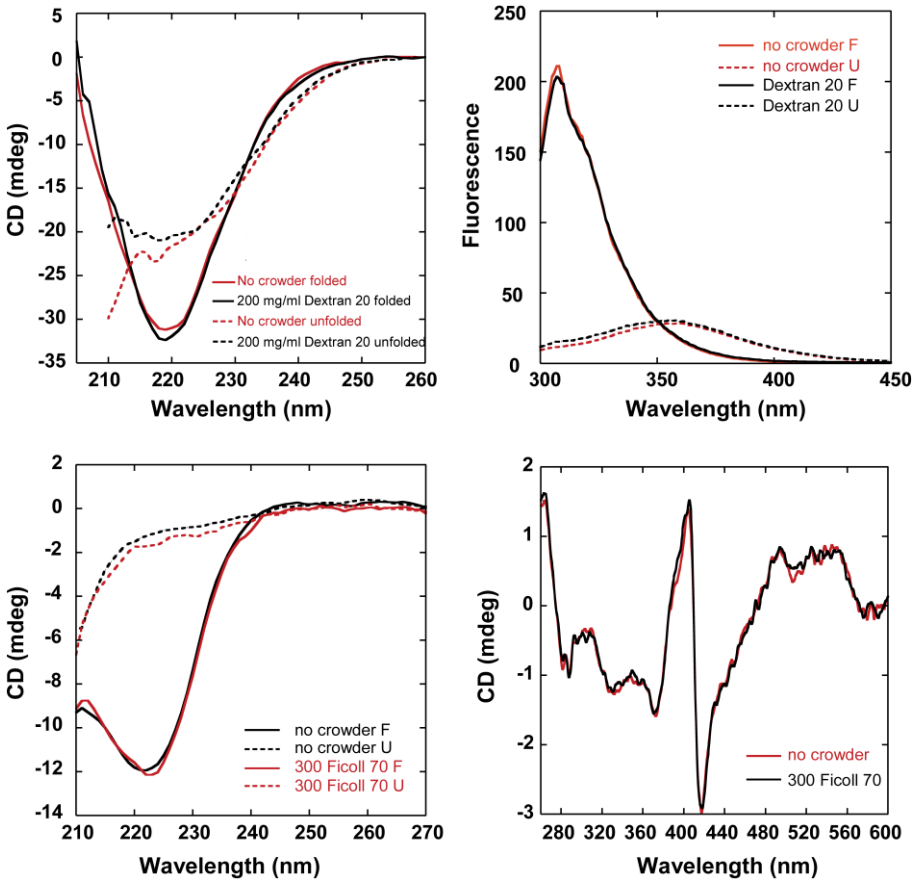

Figure 14) Effect of crowding agents on the CD and fluorescence signal of folded and unfolded apoazurin and cytochrome c. Upper panel, effect on apoazurin; left, CD spectra for folded and thermally unfolded apoazurin, right fluorescence for folded and chemically unfolded apoazurin. In both cases measurements are in buffer and in presence of 200 mg/ml Dextran 20. Lower panel, effect of crowding agents on far-UV CD signal of folded and thermally unfolded cytochrome c (left) and visible CD signal reporting on the heme group (right)

3.1.1 Cytochrome c

3.1.1.1 Thermal Unfolding of Cytochrome c

Cytochrome c is very stable towards thermal denaturation in buffer at pH 7, with a T_m of around 84 °C. Its thermal denaturation was therefore measured in increasing amounts of GuHCl to reduce its T_m. The added GuHCl

decreased the T_m and also the cooperativity (ΔH_U) of the transitions. A plot of the T_m at different GuHCl concentrations showed a linear trend and linear extrapolation to 0 M GuHCl gave the T_m in buffer/crowder as the intercept with the y-axis. A comparison of these results to those obtained using Dextran 40/70 and Ficoll 70 yields two immediate conclusions. First, the T_m at each concentration of GuHCl is clearly shifted to higher temperatures upon the addition of Dextran 40, Dextran 70 or Ficoll 70. The effect is larger for the Dextrans than for Ficoll 70 at the same mass concentration (Figure 15).

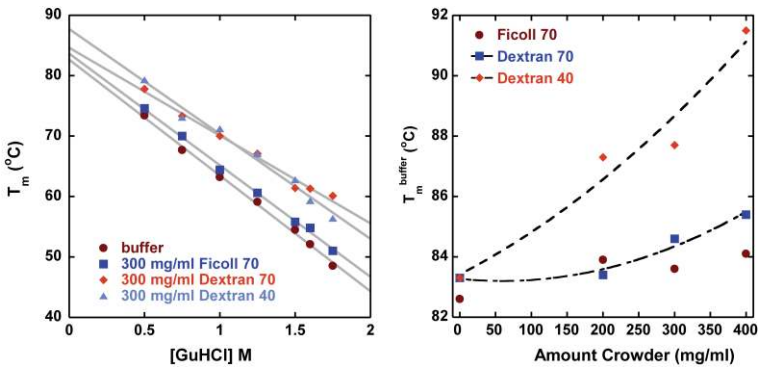

Figure 15) T_m versus GuHCl concentration for buffer, Ficoll 70 and Dextran 40/70. The lines are linear fits to the data (left). On the right, extrapolated T_ms in 0 M GuHCl as a function of increasing concentrations of Ficoll 70 and Dextran 40/70. The broken lines for both Dextrans indicate the best fitting second degree polynomials in each case.

Second, the difference in T_m increases with the crowder concentration and with the GuHCl concentration, i.e. with the destabilization of cytochrome c. At first glance, this might seem to indicate a crowding effect that increases with the initial stability of the protein. A plot of the enthalpy change for each transition against the concentration of GuHCl shows a linear decrease. The same approach as was adopted for T_m can be used to estimate the enthalpy of unfolding (ΔH_U). The enthalpy of unfolding also did not change appreciably upon addition of any of the crowders (Figure 16). Based on the estimated T_m and enthalpy changes at each GuHCl concentration, the change in free energy upon addition of crowder could be calculated at T_m (buffer). There were no trends found when $\Delta\Delta G_U$ was plotted as a function of the GuHCl concentration or buffer temperature, i.e. $\Delta\Delta G_U$ was more or less constant (see Figure 28 in the "Discussion" section). When using the Dextrans, Dextran 40 produced a stronger stabilizing effect than Dextran 70.

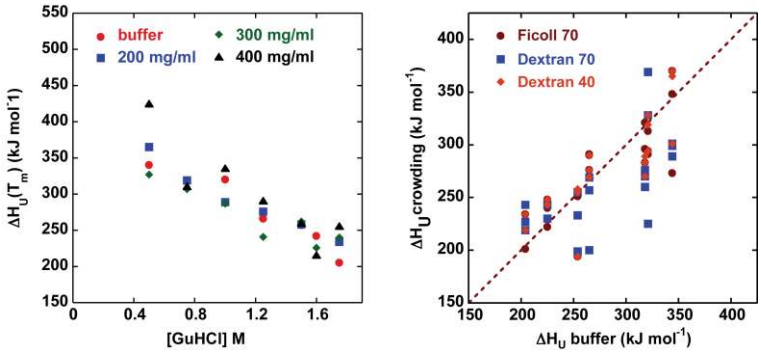

Figure 16) Plots of $\Delta H_U(T_m)$ against GuHCl concentration in buffer and solutions containing different amounts of Ficoll 70 for cytochrome c during thermal denaturation based on CD and fluorescence spectroscopy (left). Pair wise comparisons of ΔH_U in buffer and in the presence of different amounts (100- 300 mg/ml) of Ficoll 70 and Dextran 40/70 from thermal experiments. The broken line indicates the 1:1 match.(right)

3.1.1.2 Coarse-Grained Modeling of Cytochrome c

The equilibrium properties of cytochrome c under crowded conditions were simulated using a coarse-grained model. The crowders were treated either as spheres of different radii (a radius of 5.0 nm was selected to represent Ficoll 70) or as dumbbells in order to represent rods. The dumbbells consist of two spheres connected by a harmonic bond. For one dumbbell, the volume of the spheres corresponded to 2 times the volume of one Ficoll sphere. Calculations were also performed using a dumbbell for which the volume of the spheres was half the volume of the Ficoll spheres. The smallest sphere radius investigated corresponded to the size of cytochrome c. Three interesting results were obtained in the simulations. First, the smaller the crowder was in relation to the protein, the greater the stabilization. Second, spherical crowders were less stabilizing than non-spherical crowders. Third, the extension of the unfolded state decreased under all crowded conditions (Figure 17). The simulations were in good agreement with the experimental observation that Ficoll yielded less stabilization than Dextrans and also explained the greater stabilization achieved with Dextran 40 compared to Dextran 70. The degree of stabilization predicted by the simulations is considerably lower than that predicted by the models of Minton and Zhou for spherical particles (section 2.7), but the functional form of the stabilizing effect is similar to that predicted by the Minton model. The magnitude of stabilization predicted by the Zhou model is closer to that observed in the simulation,

but in this case the functional form of the simulated results is inconsistent with the output of the theoretical model.

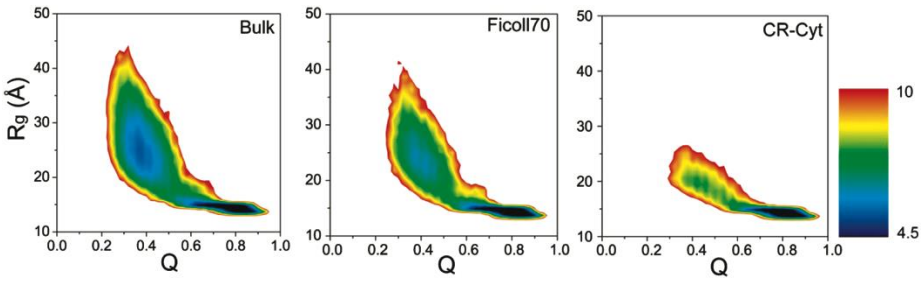

Figure 17) Folding energy landscape of cytochrome c showing the radius of gyration (R_g) as a function of the fraction of native contacts (Q) in buffer/bulk, with 40% volume occupation by Ficoll 70 or 40% volume occupation by a spherical crowder of the same size as cytochrome c (CR-Cyt). The free energy is color-coded from lowest (dark blue) to highest (red), with high values implying a low probability of finding the protein in that state

While the simulation reproduces the experimental results quite accurately, the two theoretical models only capture part of the "true picture": Minton's model predicts an overly strong effect, probably because the hard sphere assumption for the unfolded state is too strong. Conversely, the Zhou model gives too weak an effect and also does not predict the functional form of the stabilization correctly (Figure 18).

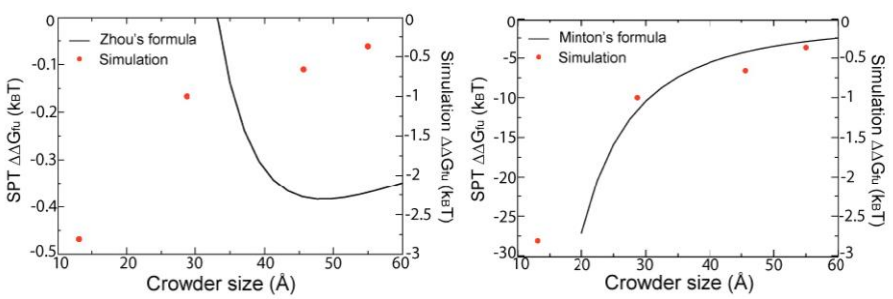

Figure 18) Comparison of MD simulation results with theoretical crowding models. The effect on the change in free engery due to crowding is plotted as a function of the size of a spherical crowder at a constant crowder concentration of 400 mg/ml. Red circle are simulation results while the continous lines are predictions from the theoretical models by Zhou (left) and Minton (right).

3.1.2 Apoazurin

3.1.2.1 Thermal and Chemical Unfolding of Apoazurin

The chemical denaturation of apoazurin with GuHCl in the presence of increasing amounts of Ficoll 70 and Dextran 20 shifted the unfolding curves towards higher GuHCl concentrations as the crowder concentration increased. The midpoint of chemical denaturation increased with the amount of added Dextran 20 or Ficoll 70. As was the case for cytochrome c, the increase was appreciably more pronounced for Dextran 20 than for Ficoll 70. Interestingly, there was a striking non-linearity in the midpoint data at concentrations higher than 200 mg/ml for both Ficoll and Dextran 20 (Figure 19).

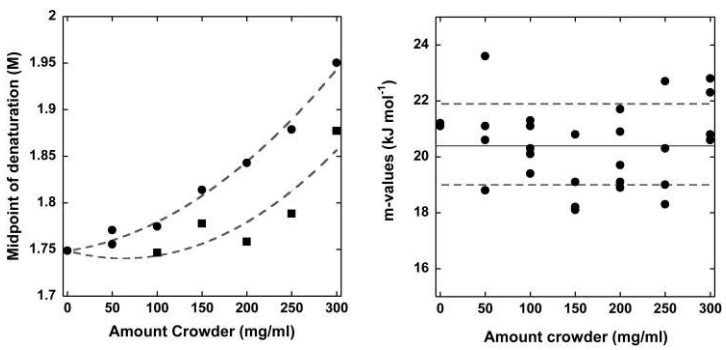

Figure 19) Left, Midpoints of the chemically-induced unfolding reactions of apoazurin in the presence of increasing concentrations of Dextran 20 (circles) and Ficoll 70 (squares). The broken lines show fitted second degree polynomials. Right, the m-values for chemically induced unfolding as a function of crowder concentration. The solid line indicates the average value and the broken lines correspond to one standard deviation.

3.1.2.2 m-values under Crowding and Free Energy Changes

To convert the measured changes in $D_{1/2}$ to ΔG_U and $\Delta\Delta G_U$ values using equation (3), a good estimate for the cooperativity of the transition is required. The m-values obtained from single denaturation curves often exhibit much fluctuation. However a plot of the m-values obtained at different crowder concentrations shows that they cluster around a value of 20.5 kJ mol^{-1} M^{-1}. In contrast to the situation for the midpoint values, the m-values did not seem to depend on the amount of added crowder. This is consistent with the findings of Batra *et al.* and Waegele and Gai[173, 174], both of whom reported that the cooperativity of the unfolding process was unaffected by

the addition of a crowder. These studies stand out as rare examples in which multiple crowders and crowding conditions were examined. In structural terms, the constant m-value suggests that the accessible surface area does not change upon unfolding. The $\Delta G_U(H_2O)$ values derived from the midpoint data and the average m-value suggest a non-linear trend that can be described with a second degree polynomial. The non-linearity sets in after 200 mg/ml and occurs when using both Ficoll 70 and Dextran 20.

3.1.2.3 Thermal Denaturation of Apoazurin

The trend observed for thermal denaturation was similar to that for chemical denaturation (Figure 20). As the amount of added crowder increases, the curves shift to a higher T_m. The effect is more pronounced for Dextran 20 than for Ficoll 70. As was the case for the m-value the ΔH_U does not appear to change upon the addition of crowder. In principal, since T_m increases in the presence of the crowder, the Δc_p should cause an increase in enthalpy. However, given the small overall shifts in T_m, this effect is lost in the noise.

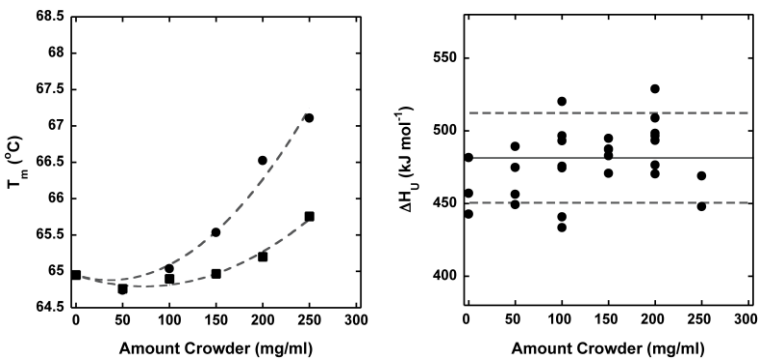

Figure 20) Midpoints of thermally-induced unfolding reactions of apoazurin in the presence of various concentrations of Dextran 20 (circles) and Ficoll 70 (squares) with best fitting second degree polynomials (broken lines), left. Right, $\Delta H_U(T_m)$ values derived from two-state fits to thermal unfolding data, respectively as a function of crowder concentration. The solid line shows the average value and the broken lines correspond to one standard deviation.

A more serious problem is irreversible protein aggregation at high temperature during thermal unfolding. The process of irreversible aggregation is dependent on the crowder concentration and also on the crowder type: Dextran 70 yielded the highest degree of aggregation and Ficoll 70 the lowest. For thermodynamic analysis, it is important that the protein is in equilibrium during the unfolding process. This was demonstrated by measuring the

unfolding curves at different scan rates (1.0 °C/ min and 0.5 °C/min), which gave identical results for T_m and ΔH_U. In addition, a 3-fold change in the protein concentration did not change the obtained thermodynamic parameters. $\Delta\Delta G_U$ can be calculated using equations (2) and (4) based on the average ΔH_U value for the unfolding process

3.1.2.4 Effect of Dextran Size on Stabilization

The use of Dextrans of varying sizes did not have any effect on the stabilization of apoazurin towards thermal or chemical denaturation at a given mass concentration. In addition, the cooperativities of the transitions from chemical and thermal denaturation did not exhibit any non-random changes, unlike the midpoint of the respective transitions. It appears that Dextran size does not affect the crowding effect of Dextran on apoazurin equilibrium stability.

3.1.2.5 Comparison of Thermal and Chemical Denaturation

Thermal and chemical denaturation both involve the unfolding process that converts the folded state to the denatured state ensemble. Assuming that the unfolded state ensemble is the same for unfolding by both means, the free energy change of unfolding should be independent of the mode of denaturation. The $\Delta\Delta G_U$ obtained from chemical (20°C) and thermal (65°C) denaturation with and without crowders correlate well with each other (Figure 21).

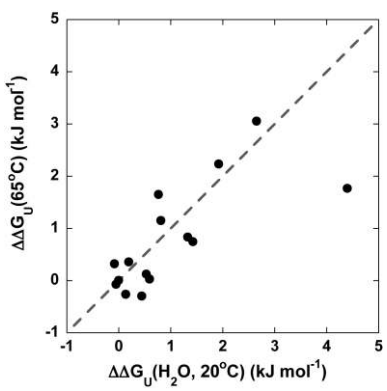

Figure 21) Pair wise comparisons of $\Delta\Delta G_U$ values obtained from chemical unfolding at 20°C (x-axis) and from thermal unfolding at 65°C (y-axis) for each particular crowder condition. The broken line corresponds to a perfect match between the two values.

The effect of macromolecular crowding on the unfolding of apo-azurin is therefore the same no matter whether measured using chemical or thermal denaturation. In addition, two probes (CD and fluorescence) were used for both perturbations, yielding comparable results. This shows that the unfolding of apo-azurin occurs via a two-state process even under crowding conditions.

3.1.2.6 Modeling of Crowding Effects on Apo-azurin

The equilibrium measurements of the thermal and chemical denaturation of apoazurin showed that its free energy of folding increased in the presence of the crowding agents Dextran or Ficoll. The degree of stabilization increased monotonically with the amount of crowder added. Ficoll 70 had a smaller effect than Dextrans of any size at the same mass concentration, and the stabilization of apoazurin was independent of Dextran size. Finally, the stabilizing effect of each crowder followed a linear trend for mass concentrations of up to 200 mg/ml but then became non-linear. Ideally, the theoretical model used to analyze experimental data should reproduce as many of the experimental properties as possible. Minton's hard-particle model uses fixed geometries for the protein and crowder (sphere and rods) and can explain the non-linearity but would predict too strong a stabilization for the Dextrans and assumes a dependence of stabilization on Dextran size. Furthermore, the effect for Ficoll would be non-linear but the non-linearity from a sphere of 2.3 nm would not be sufficient to explain the observed non-linearity. The model proposed by Zhou predicts a destabilization at higher crowder concentrations that does not fit the experimental data. The third model of Ogston and the equivalent developed by Minton that treats the crowder molecules as rods (or an array of rods) with a length much greater than the protein's radius proved to be the best candidates. Both models predict a linear response to increases in crowder concentration. An important input parameter in these models is the size of the equivalent hard sphere for the folded and unfolded state. For a sphere, this value can be calculated using the radius of gyration. The radius of gyration of the folded state can be estimated using the power law relationship proposed by Millett *et al.*[16] The parameters for the partial specific volume and the thickness of the rods were determined or taken from literature.[175] It was then necessary to decide how Ficoll should be modeled. In many cases, it has been treated as a hard sphere with a radius of 5.0 nm. However, some reports indicate that it behaves much more like an elongated molecule.[82, 83] Minton proposed that Ficoll resembled a sphericocylinder of radius 14 Å with a length to radius ratio of 7. That would imply that Ficoll is much larger in its extension than the protein

in either the folded or unfolded state. Therefore Ficoll was assumed to act like a rod.

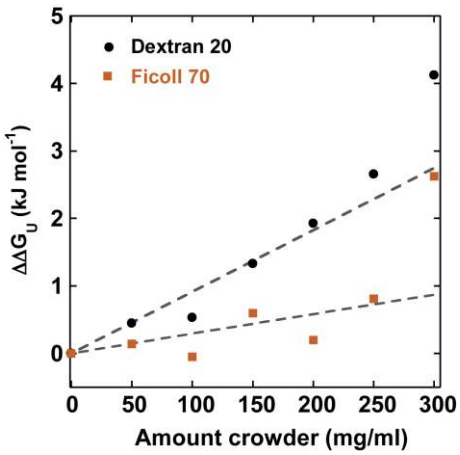

Figure 22) Application of the Ogston model to the Ficoll 70 and Dextran 20 data for the chemical denaturation of apoazurin. The data were fitted excluding the values for 250 and 300 mg/ml. The radius of gyration of the folded state was assumed to be 1.6 nm, the diameters of the crowders were 0.7 nm for Dextran 20 and 1.4 nm for Ficoll 70, and the partial specific volumes of Dextran 20 and Ficoll 70 were taken to be 0.65 ml/mg.

Using these input parameters, the model was used to fit the $\Delta\Delta G_U$ data to obtain the best fitting size for the unfolded state (Figure 22). The obtained R_g value was 20 Å for both the Ficoll and the Dextran stability data. This is a reasonable size because apoazurin contains a disulfide bridge and therefore the extension of the unfolded state will not be much greater than the folded state (16 Å). For other proteins of comparable size that also contain disulfide bridges, the determined unfolded state dimensions match the prediction for apoazurin. In addition, the fact that the same model gives the same size for unfolded azurin when used to fit the Ficoll 70 and Dextran data also suggests that the model and input parameters were well-chosen.

The use of other models is complicated by the fact that only Minton's model can describe molecules of different shapes; the models of Ogston and Zhou always assumes the crowder to be rod-like (Ogston) or spherical (Zhou). Ficoll 70 is more compact than Dextran and has been modeled as a sphere before. A comparison of the three models' output to the Ficoll 70 data (Figure 23) shows that the Zhou model cannot replicate the observed effects in magnitude or functional form. One important variable that must be estimat-

ed by the model is the length of the apoazurin chain. Because azurin contains a disulfide bridge, its length would be overestimated if one simply relied on its number of residues (128). Using a shorter chain length (104 residues) reduces the effect but is still not enough to explain the difference between model and data. The Minton model only covers some of the non-linearity, but matches the magnitude of stabilization well for a sphere of about 5.0 nm radius.Using smaller radius for the fibers in the Ogston model leads to a larger stabilization and for radii of 2.1 and 1.4 nm the model captures the magnitude of stabilization well, but this model does not reproduce the system's non-linearity.

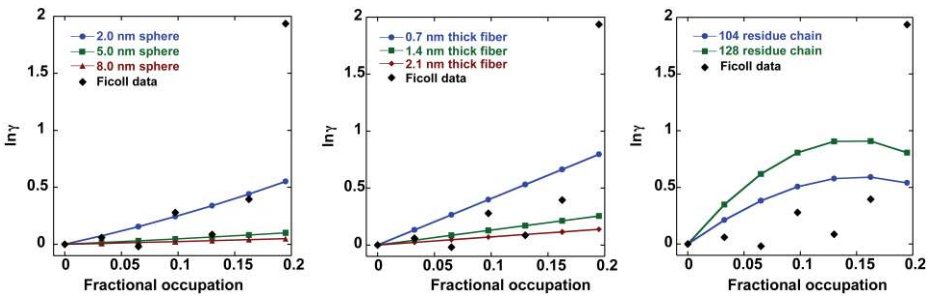

Figure 23) Application of the three crowding models to the chemical denaturation data for apoazurin in the presence of Ficoll 70. Right, model I with crowding spheres of 2.0, 5.0 and 8.0 nm radius. Middle, model II by Ogston with crowding fibers having diameters of 0.7, 1.4 and 2.1 nm. Left, model III by Zhou with chain lengths for the unfolded state of 104 and 128 residues. The folded state was in all cases assumed to be a sphere of 1.6 nm and for models I and II, the unfolded state was assumed to be a sphere of 2.0 nm radius.

3.1.3 Summary of the Equilibrium Data

The equilibrium denaturation experiments using cytochrome c and apoazurin with Dextrans of different sizes and Ficoll 70 as crowding agents yielded the following conclusions:

1) Increasing the amount of added crowder increases the magnitude of the stabilizing effect on the folded state.

2) The crowders do not change the protein's solvent exposure upon unfolding: ΔH_U and m-values do not change in the presence of any of the crowders examined.

3) Heat and chemical denaturation give comparable results in terms of $\Delta\Delta G_U$ effects of crowders.

4) The crowding effect is independent or only weakly dependent on Dextran size and always gives a stronger stabilization effect with Dextrans than Ficoll 70.

5) A simple model using rod-shaped crowders for the excluded volume can replicate the observed experimental data.

3.2 Effects of Crowding on Folding Kinetics

Folding kinetics were measured for apoazurin, apoflavodoxin and cytochrome c. In the case of apoflavodoxin, a phi value analysis was also performed to determine the effects of crowding on the folding transition state.

3.2.1 Apoazurin Folding Kinetics

Kinetic experiments on the folding of apoazurin with GuHCl as the denaturant revealed curvature in the folding and unfolding limbs of the Chevron plot. To avoid these non-linear regions, the analysis was restricted to the linear part, which corresponds to the interval where equilibrium denaturation was measured. Nevertheless, it is noteworthy that the curvature did not disappear upon the addition of the crowder. When using larger dextrans, the performance of the stopped-flow instrument deteriorated and so Dextran 20 was the only dextran crowder for which large quantities of crowder (up to 200 mg/ml) could be investigated. Since the equilibrium measurements did not reveal any dependence of the crowding effect on Dextran size, Dextran 20 was taken to be representative of the effects of Dextrans on kinetics. This assumption was supported by the fact that the chevron plots obtained using Dextran 40 and 70 at concentrations of up to 100 mg/ml were comparable to those generated using Dextran 20 data (see Figure 27 in section **3.2.4**). Dextran addition caused an increase in the observed refolding rate constants but left the unfolding rate constants unchanged. The increase in the measured refolding rate constant at different GuHCl concentrations and increasing Dextran 20 concentrations was linear. When the shift in rate constants due to crowding was converted into a $\Delta\Delta G_U$ value, the same degree of stabilization towards unfolding was obtained as in the equilibrium unfolding experiments. Furthermore the m-values for folding and unfolding were also unchanged by the addition of Dextran 20 and their sum matched the equilibrium m-value well. These results can be best explained by assuming that Dextran has an energetic effect on the unfolded state, leaving the transition and

the folded states unchanged (or changed in the same direction and by the same magnitude).

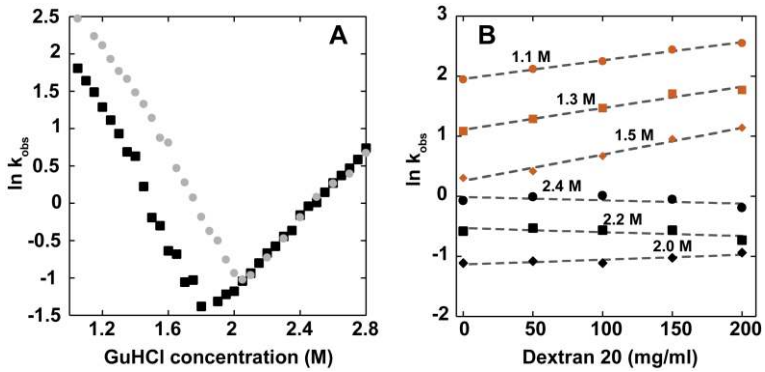

Figure 24) Folding/unfolding kinetics of apoazurin in the presence and absence of Dextran 20. A. Chevron plot ($\ln k_{obs}$ versus GuHCl concentration) without (squares) and with (circles) 200 mg/ml Dextran 20. B. $\ln k_{obs}$ as a function of Dextran 20 concentration (increasing in 50 mg/ml increments) for three GuHCl concentrations in the folding arm (1.1 M, 1.3 M, and 1.5 M) and three concentrations in the unfolding arm (2.0 M, 2.2 M, and 2.4 M) as indicated in the figure. The broken lines are linear fits to the data points.

3.2.2 Apoflavodoxin Folding Kinetics

The folding kinetics of apoflavodoxin deviated from simple two-state behavior and included an off-pathway intermediate. Phi value analyses of 13 point-mutated variants in buffer showed that the highest phi values clustered in the β-sheet region, highlighting the importance of this part in the overall folding reaction of apoflavodoxin. Information on early misfolding events was obtained by studying the burst phase in the stopped-flow experiments. The burst in CD amplitude has been traced to misfolding based on earlier simulation data.[169] It was concluded that the correct arrangement β-strands β1, β3 and β4 is the most important parameter for correct folding of apoflavodoxin.

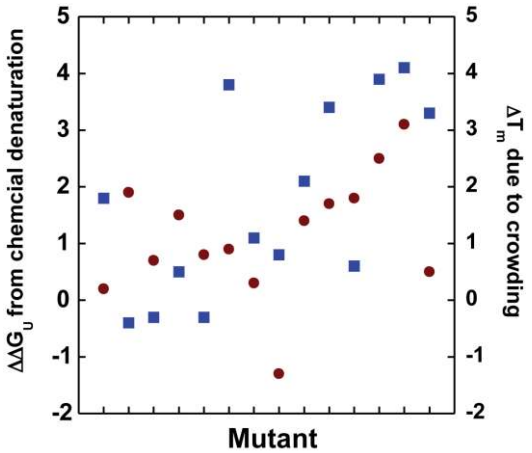

Figure 25) Comparison of the effects of adding 100 mg/ml Ficoll 70 on the stabilization against thermal (blue squares, right x-axis) and chemical (red circles, left x-axis) denaturation for the different mutants. For each mutant, stabilization against thermal denaturation correlates well with stabilization against chemical denaturation.

The addition of 100 mg/ml Ficoll 70 had two effects. The first was an increase in the equilibrium stability of apoflavodoxin variants against chemical and thermal denaturation compared to buffer conditions. The stabilizations against thermal and chemical denaturation due to crowding correlated well for each mutant, i.e. high stabilization against chemical denaturation conferred a high degree of resistance to thermal denaturation (Figure 25). Second, the folding rates of the wild type and mutants changed in response to crowding. Unlike apoazurin where the only parameter affected was the refolding rate constant, apoflavodoxin showed varied behaviors depending on the mutant. Some mutants only exhibited changes in the refolding or unfolding rate constants while others showed changes in both constants. In all cases, the effect caused an increase in the rate constants for folding and/or a decrease in the unfolding rate constant (Figure 26). For two mutants, the effect of increasing the amount of added Ficoll 70 (0 -120 mg/ml) on the refolding constant was measured and found to be linear.

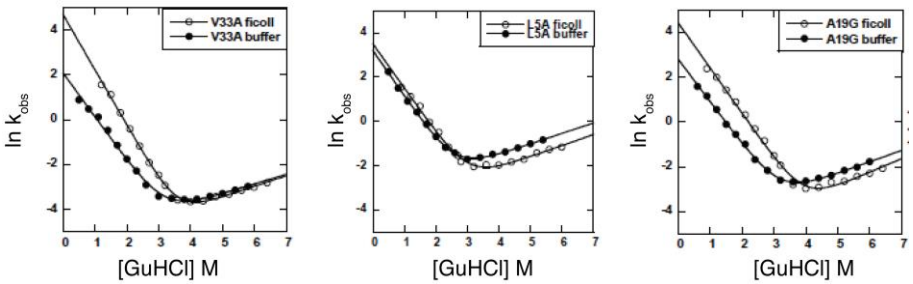

Figure 26) Individual Chevron plots for single apoflavodoxin variants showing the range of effects observed upon addition of 100 mg/ml Ficoll 70. An effect on the refolding limb only (left), the unfolding limb only (middle) or both (right).

3.2.2.1 Burst Phase and phi Values

The addition of Ficoll 70 decreased the initial burst phase of the CD signal for all mutants, indicating a lower degree of misfolding (Figure 27, left). The largest decrease in the burst phase was measured for variants with mutations in the central β-strand, residues which had previously been shown to be crucial for early folding. The excluded volume effect due to the addition of Ficoll 70 seemed to decrease the propensity of the unfolded protein chain to adopt conformations that promote misfolding. In addition, the folding phi-values for almost all mutants were reduced by the addition of the crowders (Figure 27, right).

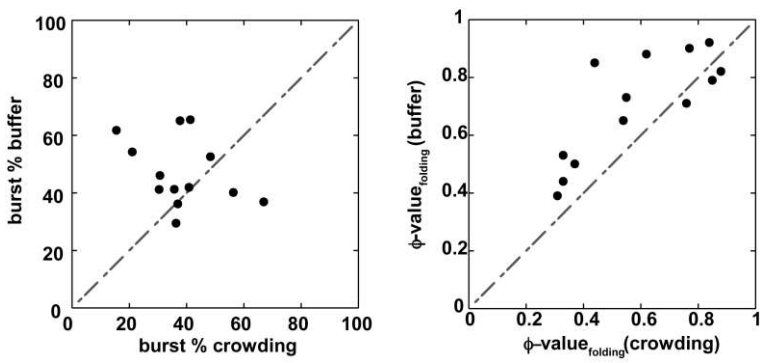

Figure 27) Left, Burst phase amplitudes as a %age of the total CD signal change at 222 nm in buffer (y-axis) compared to that in 100 mg/ml Ficoll 70 (x-axis) for all apoflavodoxin variants. Right, Φ-values obtained for all apoflavodoxin mutants in buffer (y-axis) versus 100 mg/ml Ficoll 70 (x-axis). Broken lines indicate one-to-one relationships between the x and y variables.

A decrease in the phi value due to crowding would imply that the mutated residue forms fewer interactions in the transition state in presence of crowders. This is inconsistent with the basic assumption of volume exclusion, i.e. that more compact species should be favored. However, a basic assumption of the phi value analysis is that the unfolded state remains energetically and structurally unperturbed, whereas crowding arguments assume the main effect to be on the unfolded state. To reconcile the observations with theory, one could propose that crowding-induced compaction of the unfolded state leads to a smaller difference in the reaction coordinate between the unfolded and transition state, thus leading to apparent lower phi-values for crowding compared to buffer conditions. This effect would be comparable to the Hammond effect versus ground state effects argument brought up for some proteins.[176]

3.2.3 Fast Folding Kinetics of Cytochrome c

The fast folding kinetics of reduced cytochrome c exhibited evidence of kinetic partitioning into a fast and slow folding species. The fast folding subset folds in less than 1 ms and results in a starting fraction of folded or misfolded molecules of 20 % at the first timepoint (1 μs). The addition of 220 mg/ml Dextran 70 leads to a decrease in the initial folded fraction and thus seems to eliminate the fast folding phase (Figure 28).

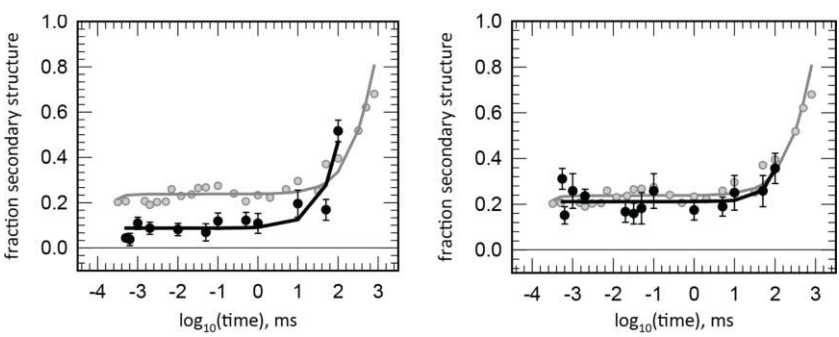

Figure 28) Fraction of secondary structure formed (estimated from CD signal at 220 nm) over time for reduced cytochrome c folding in 4 M GuHCl in the absence (gray circles) and presence (black circles) of 220 mg/ml Dextran 70 (left) and sucrose (right). The continuoues lines are exponential fits to the data points.

A possible explanation for the elimination of the fast phase might be that dextran eliminates fast folding conformations by restricting the conformational space of the unfolded polypeptide chain. The decrease in conforma-

tional space could be due to more compact conformations being more favorable for slow, correct folding. The fast folding may be caused by misligated His33-Fe-His18 coordination in the unfolded state. However, coarse-grained simulations of this coordination and unfolded protein chains with His33-Fe-His26 coordination showed that both conformations are about the same size, so the dimensions of the two different bis-His conformations cannot explain why the fast folding phase disappears in Dextran 70. It may be that the fast folding process requires access to elongated conformations on its folding pathway, which would be disfavored in the presence of Dextran 70.

3.2.4 Effect of viscosity on folding kinetics

The measured changes in kinetics are assumed to be affected by volume exclusion due to the presence of crowding agents. Hydrodynamic effects due to a change in the viscosity could potentially be responsible for the observed effects. A change in viscosity should slow down all (diffusion-controlled) kinetic processes and decrease the unfolding and refolding rates. A question that has been raised by several authors relates to the difference between micro- and macro (or bulk) viscosity.[177, 178] It has been observed that for several given proteins, the translational- and correlation diffusion time did not confirm to the Debye-Einstein and Einstein-Stokes equations.[179] While the translational diffusion decreased as expected for a given viscosity of the solution, the rotational diffusion time decreased to a lesser extent.[179, 180] The rationale behind this observation is that viscosity is defined for a hydrodynamic fluid, i.e. a continuum of solvent molecules that are much smaller in size than the solute.[177] In a crowded solution, the crowding macromolecules are about the same size as the proteins and thus the idea of a hydrodynamic fluid does not hold. The question following from the existence of both micro- and a macroviscosity is which of the two is more important to protein folding kinetics. The movements of the polypeptide governed by translational diffusion are probably less important for the folding kinetics than small, local movements that are affected by the rotational diffusion times. For the cytochrome c study, the rotational diffusion time of myoglobin was measured using linear dichroism in the presence and absence of varied quantities of Dextran 70 and sucrose. Concentrations of Dextran 20 (220 mg/ml) and sucrose (310 mg/ml) were chosen that give rise to identical rotational diffusion times and thus microviscosity. However, the two solutions differ in their bulk viscosity (or macroviscosity). The disappearance of the fast folding phase was only observed in the Dextran 70 solution but not in sucrose. This suggests that altered microviscosity is not responsible for the observed effects of Dextran 70 on the fast folding population of cytochrome c.

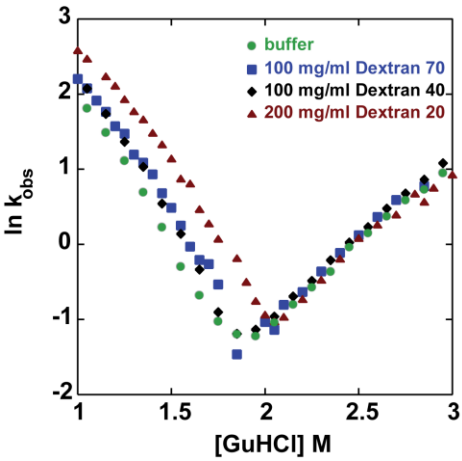

Table 2 Viscosities of Different Dextran Solutions

Dextran	Amount (mg/ml)	Viscosity (cP)
Dextran 20	100	3.3
Dextran 20	200	13.6
Dextran 40	100	4.3
Dextran 70	100	10.4

Figure 29) Chevron plots of apoazurin in presence of Dextrans of different sizes and concentrations (right). Left, measured viscosities of Dextran solutions. The viscosity of the solutions was measured on Brookfield DV-II + Pro Viscometer (Brookfield, New York) using an SC4-18 spindle at room temperature.

The fact that the effects of 100 mg/ml of Dextran 20, 40 and 70 on the unfolding and refolding kinetics of apoazurin were identical despite the clear differences in the bulk viscosities of the three solutions suggests that the observed effects probably not due to differences in viscosity (Figure 29). If the observed kinetic effects had been due to hydrodynamic effects, there should have been a clear difference between the three dextrans. Additionally, it has been demonstrated (paper IV) that the rotational diffusion time is independent of Dextran size for a range of different Dextrans (7-70 kDa), which implies that changes in microviscosity are unlikely to be responsible for the observed changes. Furthermore, if at all an increased viscosity would have been expected to *slow down* the kinetics. Oberved is however and increase in the folding rates and no effect on the unfolding rates. Based on the available data, it can be concluded that the effects on the folding kinetics of cytochrome c and apoazurin cannot be explained by differences in micro- or macroviscosity.

3.2.5 Summary of the Effects of Crowding on Folding Kinetics

The addition of crowders in the form of Dextran and Ficoll on the folding kinetics of cytochrome c, apoflavodoxin and apoazurin revealed a richer picture than had been apparent from the equilibrium experiments. In the case of apoazurin, the addition of Dextrans led to an increase in the folding rate

constants but left the unfolding rate unchanged. The rate constants for the apoflavodoxin mutants exhibited diverse behavior depending on the mutation in question, but the presence of the crowder always provided at least some degree of increased stabilization against unfolding. Furthermore, the misfolded intermediate was destabilized in the presence of Ficoll 70. For cytochrome c, the addition of Dextran caused the disappearance of the fast folding phase. In all cases, the observed effects could not be explained by differences in viscosity. Instead, the data suggest that excluded volume effects are responsible for these intriguing observations.

4. Discussion

The aim of our investigations into the role of macromolecular crowding using synthetic crowding agents *in-vitro* was to understand the forces that act on proteins *in-vivo*. The equilibrium results for cytochrome c, apoazurin and apoflavodoxin all showed a stabilization of the folded protein against either heat or chemical denaturation. In all three cases, the magnitude of stabilization increased with the concentration of added crowder and the stabilization caused by Dextran was larger than for Ficoll at the same mass concentration.

While crowding effects on protein stability have been examined in the past, most such studies focused on only one crowder at one concentration. Furthermore, the reversibility of the reaction was generally not addressed. However, based on the reported shifts in T_m due to the presence of crowding agents (Dextran, Ficoll and PEG) all of the reports published to date clearly show that crowding increases the T_m of proteins.

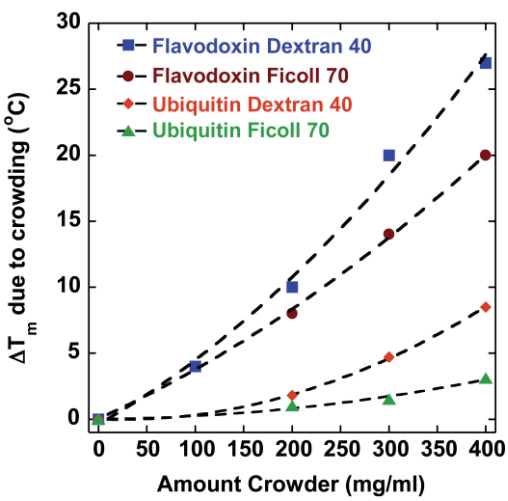

Figure 30) changes in T_m due to the addition of a crowder (Ficoll or Dextran) as function of the crowder mass concentration (mg/ml) for two proteins. The values for Ubiquitin were taken from Gai *et al.* for Dextran 40 and Ficoll 70[173]; those for apoflavodoxin are from paper 2 and Stagg *et al.*[78] The broken lines are second degree polynomials fitted to the data points.

Furthermore, the reported changes in T_m with crowder concentration usually follow a non-linear trend as was seen in this work for apoazurin and cytochrome c. In addition, where heat denaturation was performed on the same protein with both Dextran and Ficoll, it is generally found that Dextran confers a greater degree of stabilization (Figure 30). A few reports also provided the corresponding ΔH_U values, most of which indicated that crowding does not affect ΔH_U. This suggests that crowding effects are purely entropic.[103, 173, 181, 182] This is expected if the crowding agents give only rise to excluded volume effects. However, a few studies reported effects on ΔH_U due to crowding agents and the implication of these observations will be discussed in the section "Attractive Interactions".[76, 183, 184]

Chemical denaturation experiments conducted in the presence and absence of crowders typically reveal a shift in the unfolding midpoint towards higher denaturant concentrations. As with thermal denaturation, the increase becomes more pronounced as the crowder concentration increases. However, one study on holo-myoglobin reported a *decrease* in the chemical midpoint following crowder addition.[185] The effect on the m-values is not clear, but in analogy with ΔH_U in thermal experiments, the m-value should remain unchanged if the effect is purely entropic. For chemical denaturants, the effects of crowding agents on denaturant activity remain to be determined. Volume exclusion due to steric repulsion should increase the activity of all species in the system (i.e. increase the effective concentration), including the denaturant GuHCl. One way of accounting for this effect is to introduce a correction factor by calculating the available volume. This was done by deducting the solvent-excluded volume taken up by the crowders from the total volume. The underlying assumption is that the crowders are impenetrable to the denaturant molecules. This correction was applied to the activity of small species in solution in the first cytochrome c paper and has also been adopted by other groups. [100, 186, 187] This correction shifts the $D_{1/2}$ value of the chemical denaturation curve to a higher concentration while reducing the m-value and having no effect on $\Delta G_U(H_2O)$. It is not clear whether this is the right approach. The correction factor was not incorporated into the chemical denaturation data presented in this thesis.

For equilibrium unfolding experiments *in-vitro*, the change in free energy due to crowding is in the range of 4.0 kJ/mol while that in T_m is about 3.0 °C.[221] The results reported in this thesis fall within this range.

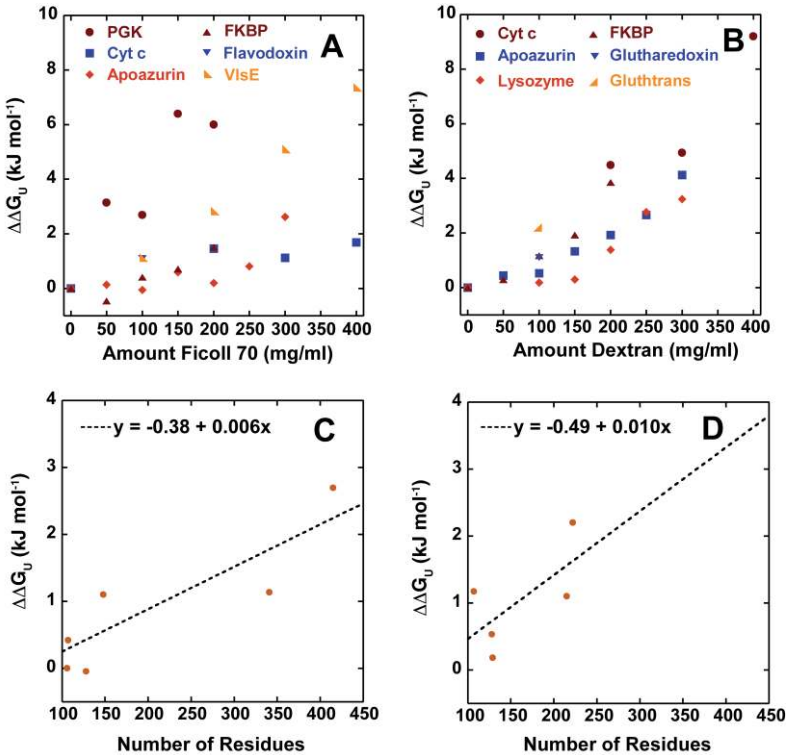

Figure 31) Collection of reported effects on protein folding equilibria as function of the amount of Ficoll 70 (A) or Dextran of any size (B). See table (x) for values and sources. Effects of stabilization as a function of protein size (in number of residues) for 100 mg/ml Ficoll 70 (C) and Dextran (D). The broken lines in C and D are linear fits to the data points.

Theoretical considerations suggest that in addition to the size and geometry of the crowders, the relative sizes of the folded and unfolded protein states and the ratio of protein to crowder size should have important impacts on the crowding effect. Larger proteins have a larger folded state but a comparatively larger unfolded state, so the effect of crowding should increase with protein size. The paucity of studies using the same crowder (or crowders) and concentrations make comparisons difficult. However, analysis of the literature data for all of the proteins that have been used in denaturation experiments in the presence of Ficoll or Dextran (on the assumption that the effects of Dextrans are independent of their size) gives Figure 31. It is clear that the crowding effect scales with the concentrations of Dextran and Ficoll, and that the effect is somewhat non-linear. For a crowder mass concentration of 100 mg/ml, there are data for more than 2 proteins in solution with

Dextran and Ficoll 70. By plotting the reported stabilizations against the length of the protein, it is clear that there is a trend towards increasing stability with increasing protein size. This effect holds for both Ficoll and Dextran, but the difference between the two crowders is quite small. This is in contrast to the observation that Dextran should be more stabilizing than Ficoll, although the effect is usually not that pronounced at 100 mg/ml. The small number of samples considered must also be taken into account in this case.

Table 3) Length and Radii of gyration (R_g) for unfolded and folded chains of proteins listed in figure 31 and sources of the crowding data

Protein	Length	Fold	R_g^F (nm)	R_g^U (nm)	Reference
PGK	415	α	2.5	7.4	Dhar *et al.*[103]
Lysozyme	129	α/β	1.6	2.3	Sasahara *et al.*[181]
FKBP	106	α/β	1.5	3.3	Spencer *et al.*[188]
VlsE	341	α	2.3	6.6	Perham *et al.*[102]
Glutharedoxin	215	α/β	2.0	5.0	Kuhnert *et al.*[189]
Flavodoxin	148	α/β	1.7	4.0	Stagg *et al.*[78, 189]
Cytochrome c	104	α	1.4	3.0	Paper I
Apoazurin	128	β	1.6	2.0	Paper II
Glutatransferase	222	α	2.0	5.1	Kuhnert *et al.*[189]

* Values for the radius of gyration (R_g) were calculated according to the power law in Millett *et al.*[16] For cytochrome c, the values are taken from Segel *et al.*[190] and those for lysozyme are from Millett *et al.*[191].

4.1 Attractive Interactions?

The presented models assume only repulsive steric interactions between crowders and protein. The possibility of attractive interactions between protein and crowders has been proposed and might explain the discrepancies between different experimental data sets.[71, 72, 192] Since Ficoll and Dextran are uncharged molecules, ionic interactions with proteins are not expected. Studies have indicated that unlike PEG [73, 74], Ficoll and Dextrans do not form specific interactions with some proteins. However, this claim has recently been questioned.[71, 112, 192] One way of investigating the existence of an enthalpic component is to probe for a temperature dependence of the crowding effect according to (4). The change in the free energy of unfolding due to

crowding can be split into enthalpic and entropic contributions according to (23).

$$\Delta\Delta G_U = -RT \ln(K_{crowded}/K_{buffer}) \quad (23)$$

This expression can be substituted to yield (24):

$$\ln(K_{crowded}/K_{buffer}) = -\Delta\Delta H_U/RT + \Delta\Delta S_U/R \quad (24)$$

According to equation (24), enthalpic contributions due to attractive interactions that favor the unfolded state should cause $\ln(K_{crowded}/K_{buffer})$ to decrease with decreasing temperature.

Jiao *et al.* reported that the crowding effects of Ficoll and PEG on the association between SOD and catalase depends on the temperature and concluded that an enthalpic component exists in that system[92]. However in a study on the interaction between bovine serum albumin (BSA) and Ficoll using equilibrium sedimentation, no temperature dependence of the observed changes in buoyant mass was observed and so it was concluded that only entropic effects were relevant in this case [83]. However, a temperature dependence was observed for protein crowders.[193] The Pielak group reported that the ΔH_U values for CI2 and ubiquitin changed following the addition of crowders (PVP, Ficoll) and interpreted that as a consequence of non-specific attractive crowder-protein interactions.[76, 183, 184]

For the proteins studied in this thesis work, cytochrome c and apoazurin, the available data do not indicate that the crowding effect is temperature dependent (Figure 32). The chemical denaturation of apoazurin was performed at 20 °C while the thermal denaturation was measured at around 65 °C. The changes in the K_U values for these two methods following the addition of Ficoll or Dextran were very similar. If attractive interactions were present, the two values should have been different, with a more pronounced stabilizing effect at 65 °C than at 20 °C. For cytochrome c, conversion of the measured T_m and ΔH_U values to ΔG_U, $\Delta\Delta G_U$ (crowding-buffer) and K_U also did not reveal any change in the ratio of $\ln K_U$ with temperature. Based on these results, we conclude that the temperature did not measurably affect the stabilization provided by crowding agents. This suggests that there are no attractive crowder-protein interactions in the studied systems and supports the conclusion of purely steric repulsions between the crowding agents and protein systems considered.

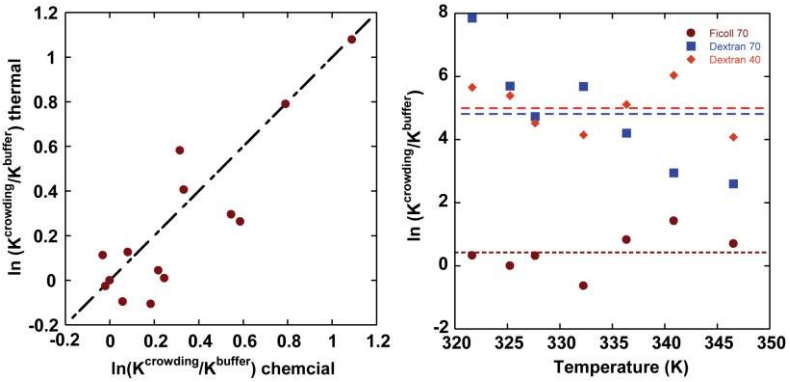

Figure 32) Effect of temperature on the ratio of the equilibrium constant with crowding to that in buffer. On the left: pair wise comparison of each crowder condition using thermal (T_m around 65 °C) and chemical (20 °C) denaturation. The broken line shows a 1:1 match. On the right: the logarithmic ratio of the equilibrium constants with and without crowding for cytochrome c at different temperatures. The $\Delta\Delta G_U$ values used for conversion were calculated using the average ΔH_U at each [GuHCl] from figure (14). The broken lines indicate the average value for each crowder over the temperature range.

Overall, when considered in conjunction with previously published findings, the results presented herein strongly suggest that the crowding agents Dextran and Ficoll 70 stabilize proteins against heat and chemical denaturation. Moreover, at a given mass concentration, Dextran has a greater stabilizing effect than Ficoll 70. This may be due to the thinner rod shape of Dextran compared to Ficoll. The magnitude of stabilization is usually modest (1-3 kJ/mol; 1-5 °C). Based on the studies of apoazurin and cytochrome c, it appears that the effects of Ficoll and Dextran were purely due to steric repulsion. The overall magnitude of stabilization due to crowding is small and one may be tempted to ask whether such small effects are significance under *in-vivo* conditions. However, the reactions within a cell are finely tuned and even small changes due to processes such as mutation can have drastic consequences. The p53 transcription factor is only marginally stable and small differences in stabilization caused by a single mutation that reduces its stability could have adverse effects such as an elevated probability of cancer.[194] In another example, Walkiewicz *et al.* found in a mutant analysis of the tetracycline resistance protein TetX2 that a two-fold change in K_m was enough to cause considerable antibiotic resistance.[195] Finally, it has been shown that

very small changes in affinity of hemoglobin for O_2 can have significant effects on activity.[196] It should also be noted that to date, only effects on single proteins have been considered. Reactions within a cell usually occur as parts of a larger network, and small effects in one link could have important upstream consequences. Minton et al. have argued that, for example, activity changes due to slight changes in cellular volume could lead to a strong response in the transport flux over a membrane in a hypothetical transport system.[197]

These examples illustrate how narrowly stabilities and activities are tuned and how even small perturbations, such as those due to crowding, can have strong effects.

4.2 Crowding Effects on Kinetics

Only a few reports have addressed the effects of crowding agents on protein folding kinetics. For simple two-state kinetic reactions, the effects of crowding on the folded, unfolded and transition states need to be considered. For more complex folding reactions, intermediate structures and/or parallel pathways must also be taken into account. Excluded volume effects should be most unfavorable for the more expanded unfolded state, followed by the transition and finally the folded state. This should result in faster refolding rates and invariant or slower unfolding rates. The effects on unfolding rates depend on how the compaction of folded and transition states differ. For apoazurin and apoflavodoxin, the T_β is ~0.65, implying that the transition state is close to the folded state in terms of compaction/interactions. In keeping with this conclusion, crowding has a noticeable effect on the refolding of apoazurin but the unfolding rate is unaffected. Reports from other groups have shown that the folding rate constant for apocytochrome b562[112] is increased in the presence of 100 mg/ml PEG while the unfolding rate constant is unaffected, and similar results have been reported for VlsE in the presence of Ficoll 70 at mass concentrations of up t0 100 mg/ml[110]. However, for the ribosomal protein S16, both the folding and unfolding rate constants changed upon the addition of 200 mg/ml Dextran 20. [101]

Our time-resolved studies indicated that folding is not a two-state process for apoflavodoxin and cytochrome c. There is a misfolded burst intermediate of apoflavodoxin that becomes less populated under crowded conditions. It was suggested that this happens because the unfolded state is more compact in crowded conditions and that this biases the reaction towards productive folding. In keeping with this hypothesis, coarse-grained simula-

tions showed that unfolded apoflavodoxin is more compact and forms more native interactions in the presence of crowders. For cytochrome c, less fast folding is observed on the μs timescale in the presence of crowders. Instead, cytochrome c molecules all fold homogenously to the folded state via a slower reaction under crowded conditions. The proposed explanation is similar to that for apoflavodoxin: it is suggested that the unfolded state has a compaction bias that pushes the reaction in a certain direction. It is still unclear whether the fast μs-scale phase of cytochrome c corresponds to correct folding or misfolding. While the observed effects could be due to heme misligation in the unfolded state, *in-silico* data suggest that this is not the case.

Two reports by Monterroso and Minton as well as van den Berg *et al.* reached a conclusion similar to that presented here. In the former study, the refolding speed (measured in terms of the gain in catalytic activity) of carbonic anhydrase was probed in the presence of up to 150 mg/ml Ficoll 70. An increase in the refolding rate was observed, but at the same time the total amount of refolded protein decreased under crowding. The authors proposed that a non-productive protein conformation formed to a larger extent under crowded conditions.[107] Van der Berg *et al.* found that the refolding speed of reduced lysozyme in 80 mg/ml Ficoll 70 increased, but at the same time they observed a lower yield of correctly folded lysozyme. Their explanation for the lower yield was a higher propensity for aggregation of reduced lysozyme in the presence of Ficoll 70.[108, 109]

In summary, the effects of crowding agents on the folding kinetics of proteins are (1) increased rate constants of folding (due to destabilization of the unfolded state) and (2) mechanistic changes and/or bias towards certain folding pathways due to the altered ensemble of unfolded chain conformations.

4.3 *In-vitro* vs *In-vivo* Conditions

The discussion so far has centered on how excluded volume effects can be mimicked *in-vitro* using crowding agents such as Ficoll or Dextran. What does this tell us about *in-vivo* conditions? In cells, more factors affect proteins, such as viscosity and non-specific interactions. Moreover, *in-vivo*, the protein ensemble has a large distribution of different sizes and shapes, which contribute to the excluded volume effects. In *E. coli*, the average protein length is estimated to be around 325 amino acids.[198] This is larger than the proteins used in most studies of *in-vitro* model systems to date but still smaller than most crowding agents. Dill *et al.* have concluded that the major-

ity of all proteins in the *E. coli* proteome have a stability (ΔG_U) of about 28 kJ/mol at 37 °C. Thus even a modest increase in stability due to crowding may have a significant effect on the survival of the proteome during stress conditions.[199]

It is difficult to perform experiments inside cells, partly because all of the factors present in the cell can contribute to the results.[200] This challenge has nevertheless been taken up by some groups. Ghaemmaghami and Oas measured the stability of λ suppressor both *in-vitro* and inside *E. coli* cells, using urea as denaturant and monitoring the process via hydrogen exchange measured by Matrix-assisted laser desorption/ionization (MALDI). They reported that the stability measured *in-vivo* did not deviate form the-*in vitro* values.[201] In contrast, Gierasch measured the stability of retinoic acid-binding protein (CRAB) in *E. coli* cells against urea denaturation using FRET. They found that the protein is destabilized *in-vivo* and that both its midpoint and m-values are smaller than the corresponding *in-vitro* values.[202, 203] Using temperature jumps, *Dhar et al.* measured the folding kinetics and stability of FRET-labeled PGK in different cell compartments (ER, cytosol, nucleus). They found that PGK was slightly stabilized against heat denaturation and the folding kinetic effects depended on the cell compartment in which PGK was situated.[103, 204] High resolution structure determination in cells is difficult, but progress in NMR has yielded preliminary results as discussed in two review articles.[205, 206] *Sakakibara et al.* succeeded in determining the structure of TTHAI1718, a metal-binding protein, in *E. coli*. The resulting structure was very similar to the *in-vitro* structure, but showed differences in a few loop regions.[207] A completely different result was observed for FlgM, an intrinsically disordered protein that becomes structured in *E. coli*. The same was observed *in-vitro* upon addition of 400 mg/ml bovine serum albumin or glucose.[208] For eukaryotic systems, one way of performing such studies involves microinjection into oocytes of *Xenopus laevis*. This approach has been used by Bodart *et al.* for the human neuronal protein Tau, which binds and stabilizes microtubules of the cytoskeleton, and is also intrinsically disordered. The conformation of Tau in *Xenopus* oocytes did not differ detectably from that seen *in-vitro*.[209] For mammalian cells, the challenge was even greater, but early attempts yielded NMR spectra that were not too different from *in-vitro* recordings. While a few residues appeared to have changed, this may have been due to modifications of the amino-acid residues in many cases.[210-212] The measurement of *in-vivo* protein structures is still in its early stages, but so far it seems that the overall folded structure *in-vivo* is similar to that *in-vitro*.

Viscosity differences between *in-vivo* and *in-vitro* environments are another factor that must be considered. The studies on folding kinetics for cytochrome c and apoazurin highlighted the potential viscosity effects caused by crowding. However, the results obtained suggested that changes in viscosity were not responsible for the measured effects. The viscosity of Dextran and Ficoll solutions is considerably higher than that of pure water. However, measurements of the viscosity of the cytoplasm using a range of different techniques such as single particle tracking (SPR)[213], fluorescence recovery after photobleaching (FRAP)[214, 215], and fluorescence correlation spectroscopy (FCS)[216, 217] all suggested that the diffusion speed of molecules in the cytoplasm is only a few times slower than in pure water, and much lower than in the crowder solutions.[177] A larger difference that has been reported is hindered diffusion, i.e. fractions of molecules have been observed to diffuse differently to others. This was related to membranes or sieving effects of the cytoskeleton.[218] Based on viscosity measurements in the cytoplasm, it appeared that the viscosity is only about 3-times higher than that of pure water and was less restrictive than one might expect given the large number of macromolecules present.[43, 177, 219, 220] Given that solutions containing crowding agents have much higher viscosities, it seems likely that the observation of folding kinetics acquired using crowding agents at high viscosities will also be valid in the less viscous cytoplasm.

Thus, *in-vivo* experiments definitely provide information about how proteins fold in the context of the cytoplasm, but it is difficult to discern what factors influence the observed behaviors or the magnitude of their effects. The approach presented here involves studying one effect at a time (here, volume exclusion due to steric repulsion) by careful and systematic experimentation *in-vitro*.

5. Conclusion and Summary

This study sought to elucidate the effects of the macromolecular crowding agents Ficoll and Dextran on the folding equilibria and kinetic folding reactions of three proteins. The addition of crowding agents led to a concentration-dependent stabilization of all three proteins against heat and chemical denaturation. In all cases, the protein stabilization due to Ficoll was smaller than that for Dextran at the same mass concentration. The stabilization effects were shown to be independent of temperature, ruling out enthalpic contributions, and simple excluded volume theory could reproduce the effects. The role of the crowders' geometry remains unclear: for apoazurin, modeling that treated Ficoll and Dextran as rods explained the observed stabilization well while for cytochrome c, modeling Ficoll as a sphere was sufficient. The studies show that Ficoll and Dextran can be used as crowding agents to mimic volume exclusion exclusively.

The folding kinetics for apoazurin were faster in the presence of crowding agents but its unfolding rate was unchanged. The two-state folding mechanism remained unchanged by crowding. Apoflavodoxin and cytochrome c did not fold via a two-state kinetic process, and crowding also influenced their folding mechanisms and their channeling between pathways. For cytochrome c and apoflavodoxin, it was shown that the kinetic effects were not due to changes in the viscosity of the solution. The kinetic experiments showed that macromolecular crowding speeds up folding by reducing the unfolded state entropy and that these unfolded state effects reduce the population of mis-folded species.

6. Outlook

The results of this thesis and related investigations have shown that Ficoll and Dextrans can be used as crowding agents. Their effects can be described in terms of volume exclusion alone, without needing to consider any specific attractive interactions. However, Ficoll and Dextrans needed to be modeled as long rods, with the only difference between them being that one is thicker than the other. This implies that some of the most widely cited and discussed models of crowding do not capture the effects of Dextran and Ficoll. Future experiments in this area should arguably focus on two lines of investigation, one dealing exclusively with the Ficoll/Dextran systems and the other looking at crowding in a more general sense.

Attractive crowder-protein interactions have been proposed to occur in Ficoll and Dextran systems, although many cases exist where pure steric repulsion was sufficient to explain the observed effects. The nature and origin of these attractive interactions remains unclear, especially because the basic chemistry of all proteins is identical. One way of investigating these interactions would be to measure crowding effects over wide temperature ranges as opposed to the usual short temperature intervals. Additionally, the effect should scale with the size of the protein.

Considering the experimental techniques used in this work, it might be interesting to conduct classical colligative experiments, i.e. ultracentrifugation and osmotic or vapor pressure analyses. Ultracentrifugation has been used to measure activity coefficients for association equilibria, but unfolding equilibria have not been investigated. It could potentially enable measurement of the activity coefficients of the unfolded and folded state in the presence of crowders.

In principal, colligative techniques could be applied to protein crowders as well. *In-vivo* studies have shown that proteins are either not affected at all by such techniques and may even be slightly destabilized. Sometimes this is seen as proof that crowding has less of an effect or is unimportant in the *in-vivo* than expected. Still, these experiments do not explain why the stability is as observed. On the contrary, it just raises another question, what destabilizes the protein so much as to cancel out these repulsive effects? By bearing the findings from *in-vitro* crowding studies with crowding agents in mind,

protein crowding systems could be studied with a much stronger focus on non-specific attractive interactions.

Another experimental approach that has been only used to a small degree in this field to date is NMR. At present, only one group has used this technique to elucidate crowding effects. NMR too could allow the study of systems with protein crowders, since labeling of proteins could render the background protein basically invisible. The residue-specific resolution together with colligative techniques might give new insights into the thermodynamic parameters underlying protein properties in crowded environments.

Acknowledgements

So, after almost 5 years it is nearly done. Altough the thesis has to be defended by me alone there are still a whole bunch of persons who more or less directly took part in it. Be it by being involved in the experiments or by helping to make the time more pleasant.

At first place I would like to thank my supervisor Pernilla, afterall thanks to you I actullay could do my work in macromolecular crowding. After you recruitment talk in Umea I was already interested in crowding and I was quite happy the moment in your office when we talked about a project for my then masterthesis that you directly suggested crowding. I want to thank for your help, input and advice on my research and experiments. We for sure had to crack here and there some tough nuts with the crowding stuff. Also besides research it was always pleasent talking to you and you were always willing to share a lot of information about how science, funding and publishing works. I admire your way of writing articles and also your determination as soon as the critical mass for publication has been reached. While others might then need another year before something more has happened, in your case that is focused and done!

Next is my second supervisor Magnus. My interest on protein folding was awakended during your 'Protein Structure and Function' course, plus you gave extra points on the exam if we visited Pernillas' lecuture. Also, my thanks for your input and ideas during all the years.

I would also like to thanks the rest of my committee Dan and Ove for your patience and discussions during the sometimes somewhat lengthy yearly evaluations. A vague guess from my side: the actual defence will be shorter than the last evaluation.

Of course I would like to mention and thank my research group, past and present members. Especially I would like to thank the "original" three Maria, Moritz and Ximena. Maria besides working together and later as office mates we had a lot of funny and sometimes not so funny conversations about work, life and ,of course, the news on "People Magazine". During the years you were a great help, a good listener and a good friend! I wish you all the best for your future and hope we stay in touch! Ximenita, muchas gracias por el tiempo como compadre en nuestra oficina i nuestras conversaciónes más o

menos científicas i que tengas suerte con la defensa tuya! Also thanks to our post-docs Jörgen and Istavan (egészségedre!).

Yo Mo, danke für die super Zeit. Hat ja schon gleich beim ersten Treffen „gefunkt“ und jemand der Alpha Centauri kennt, kann ja nur ein guter Mensch sein, oder? Vielen Dank und Grüße auch an deine Frau Hanna und die kleine Herja und den weiteren Zuwachs (Kevin oder David?). Grüße auch an den Rest der deutschen Mafia: Constantin und Familie, Mark, Lena und Familie und Manuela und seit kurzem dazugestossen Dana und Michael (hättet mal früher kommen sollen).

Tack Johan för en introduktion till ölbryggning och dem tillfällen när du och Karin tog hand om en ensam kille pa nyårsafton! Marcus… tack för att lära mig vara ödmjuk… 5 år och inte en enda gång har jag vunnit i våra squash matcher. Samuel som jag tackar för att ha varit tandem partner, squah motståndare och också för fika och alla samtal genom nin tid i Umeå!

Also I would like to acknowledge the rest of the biophyscial corridor. Here especially P.O.for all conversations about science, actual research and ethics. Also Tobias, who has always a great help in scientific questions, and Lars Backman, I liked your course about protein purification and that was one of the reasons that I decided to stay in Umeå in the first place, even before finally starting my PhD.

Last but not least thank you Xiaowei for all your help, especially during the last part of the thesis and for the translation of the poem. I just hope you did not by “accident” introcduce any “funny” characters; it might still take some time before I will be able to spot that.

All in all thank you all for the time and all the best for the future!

References

1. Alberts, B., Johnson, A., Lewis, J., Raff, M., Roberts, K., and Walter, P. 2002. Molecular Biology of the Cell, 4th edition. Garland Science, New York.

2. Feldman, D. E., and J. Frydman. 2000. Protein folding in vivo: the importance of molecular chaperones. Current Opinion in Structural Biology 10:26-33.

3. Ulrich Hartl, F., and J. Martin. 1995. Molecular chaperones in cellular protein folding. Current Opinion in Structural Biology 5:92-102.

4. Gomes, C. M., Wittung-Stafshede P. (eds.). 2011. Protein Folding and Metal Ions- Mechanisms, Biology and Disease. Boca Raton, FL : CRC Press.

5. Marion, D. 2013. An introduction to biological NMR spectroscopy. Mol Cell Proteomics.

6. van Heel, M., B. Gowen, R. Matadeen, E. V. Orlova, R. Finn, T. Pape, D. Cohen, H. Stark, R. Schmidt, M. Schatz, and A. Patwardhan. 2000. Single-particle electron cryo-microscopy: towards atomic resolution. Q Rev Biophys 33:307-369.

7. Berova N., N. K., Woody R.W. Circualar Dichrosim Principles and Applications. Wiley-VCH, Canada.

8. Royer, C. A. 2006. Probing protein folding and conformational transitions with fluorescence. Chem Rev 106:1769-1784.

9. Nemecek, D., J. Stepanek, and G. J. Thomas. 2001. Raman Spectroscopy of Proteins and Nucleoproteins. In Current Protocols in Protein Science. John Wiley & Sons, Inc.

10. Barth, A., and C. Zscherp. 2002. What vibrations tell us about proteins. Q Rev Biophys 35:369-430.

11. Rose, P. J. F. a. G. D. 2005. Conformational Properties of Unfolded Proteins. Protein Folding Handbook. Wiley-VCH, Weinheim.

12. Dill, K. A., and D. Shortle. 1991. Denatured states of proteins. Annu Rev Biochem 60:795-825.

13. Greene, R. F., and C. N. Pace. 1974. Urea and Guanidine Hydrochloride Denaturation of Ribonuclease, Lysozyme, α-Chymotrypsin, and β-Lactoglobulin. Journal of Biological Chemistry 249:5388-5393.

14. C., T. 1968. Protein Denaturation. Advances in Protein Chemistry 23:121-282.

15. Dyson, H. J., and P. E. Wright. 2004. Unfolded Proteins and Protein Folding Studied by NMR. Chemical Reviews 104:3607-3622.

16. Millett, I. S., S. Doniach, and K. W. Plaxco. 2002. Toward a taxonomy of the denatured state: small angle scattering studies of unfolded proteins. Adv Protein Chem 62:241-262.

17. Meier, S., M. Blackledge, and S. Grzesiek. 2008. Conformational distributions of unfolded polypeptides from novel NMR techniques. The Journal of Chemical Physics 128:-.

18. Nodet, G., L. c. Salmon, V. r. Ozenne, S. Meier, M. R. Jensen, and M. Blackledge. 2009. Quantitative Description of Backbone Conformational Sampling of Unfolded Proteins at Amino Acid Resolution from NMR Residual Dipolar Couplings. Journal of the American Chemical Society 131:17908-17918.

19. Haran, G. 2012. How, when and why proteins collapse: the relation to folding. Curr Opin Struct Biol 22:14-20.

20. Millet, I. S., S. Doniach, and K. W. Plaxco. 2002. Toward a taxonomy of the denatured state: Small angle scattering studies of unfolded proteins. Unfolded Proteins 62:241-262.

21. Flory, P. J. 1953. Principles of Polymer Chemistry. Configuration of Polymer Chains:399-425.

22. Flory P. J., F. S. 1965. Effect of Volume Exclusion on the Dimensions of Polymer Phains. Journal of Chemical Physics 44:2243-2247.

23. Garcia, P., L. Serrano, D. Durand, M. Rico, and M. Bruix. 2001. NMR and SAXS characterization of the denatured state of the chemotactic protein CheY: implications for protein folding initiation. Protein Sci 10:1100-1112.

24. Kazmirski, S. L., K. B. Wong, S. M. Freund, Y. J. Tan, A. R. Fersht, and V. Daggett. 2001. Protein folding from a highly disordered denatured state: the folding pathway of chymotrypsin inhibitor 2 at atomic resolution. Proc Natl Acad Sci U S A 98:4349-4354.

25. Sherman, E., and G. Haran. 2006. Coil–globule transition in the denatured state of a small protein. Proceedings of the National Academy of Sciences 103:11539-11543.

26. Merchant, K. A., R. B. Best, J. M. Louis, I. V. Gopich, and W. A. Eaton. 2007. Characterizing the unfolded states of proteins using

single-molecule FRET spectroscopy and molecular simulations. Proceedings of the National Academy of Sciences 104:1528-1533.

27. Tezuka-Kawakami, T., C. Gell, D. J. Brockwell, S. E. Radford, and D. A. Smith. 2006. Urea-Induced Unfolding of the Immunity Protein Im9 Monitored by spFRET. Biophysical Journal 91:L42-L44.

28. Kohn, J. E., I. S. Millett, J. Jacob, B. Zagrovic, T. M. Dillon, N. Cingel, R. S. Dothager, S. Seifert, P. Thiyagarajan, T. R. Sosnick, M. Z. Hasan, V. S. Pande, I. Ruczinski, S. Doniach, and K. W. Plaxco. 2004. Random-coil behavior and the dimensions of chemically unfolded proteins. Proceedings of the National Academy of Sciences of the United States of America 101:12491-12496.

29. Yoo, T. Y., S. P. Meisburger, J. Hinshaw, L. Pollack, G. Haran, T. R. Sosnick, and K. Plaxco. 2012. Small-Angle X-ray Scattering and Single-Molecule FRET Spectroscopy Produce Highly Divergent Views of the Low-Denaturant Unfolded State. Journal of Molecular Biology 418:226-236.

30. Dill, K. A. 1990. Dominant forces in protein folding. Biochemistry 29:7133-7155.

31. Privalov, P. L., and S. J. Gill. 1988. Stability of protein structure and hydrophobic interaction. Adv Protein Chem 39:191-234.

32. Fersht, A. 1999. Structure and mechanism in protein science. A guide to enzyme catalysis and protein folding. Freeman Co, New York.

33. Levinthal, C. 1969. How to fold Graciously. Mossbauer Spectroscopy in Biological Systems: Proceedings of a meeting held at Allerton House, Monticello, Illinois:22-24.

34. Dill, K. A., S. Bromberg, K. Yue, K. M. Fiebig, D. P. Yee, P. D. Thomas, and H. S. Chan. 1995. Principles of protein folding--a perspective from simple exact models. Protein Sci 4:561-602.

35. Kuwajima, K. 1989. The molten globule state as a clue for understanding the folding and cooperativity of globular-protein structure. Proteins: Structure, Function, and Bioinformatics 6:87-103.

36. Wetlaufer, D. B. 1973. Nucleation, Rapid Folding, and Globular Intrachain Regions in Proteins. Proceedings of the National Academy of Sciences 70:697-701.

37. Kim, P. S., and R. L. Baldwin. 1982. Specific intermediates in the folding reactions of small proteins and the mechanism of protein folding. Annu Rev Biochem 51:459-489.

38. Eyring, H. 1935. The Activated Complex in Chemical Reactions. Journal of Chemical Physics 3:107-115.

39. Fersht, A. R. 1995. Characterizing transition states in protein folding: an essential step in the puzzle. Current Opinion in Structural Biology 5:79-84.

40. Fersht, A. R., A. Matouschek, and L. Serrano. 1992. The folding of an enzyme: I. Theory of protein engineering analysis of stability and pathway of protein folding. Journal of Molecular Biology 224:771-782.

41. Jester, J. V. 2008. Corneal crystallins and the development of cellular transparency. Seminars in Cell & Developmental Biology 19:82-93.

42. Minton, A. P. 1981. Excluded volume as a determinant of macromolecular structure and reactivity. Biopolymers 20:2093-2120.

43. Partikian, A., B. Olveczky, R. Swaminathan, Y. Li, and A. S. Verkman. 1998. Rapid diffusion of green fluorescent protein in the mitochondrial matrix. J Cell Biol 140:821-829.

44. Cremer, T., M. Cremer, S. Dietzel, S. Müller, I. Solovei, and S. Fakan. 2006. Chromosome territories--a functional nuclear landscape. Curr Opin Cell Biol 18:307-316.

45. Luby-Phelps, K. 2000. Cytoarchitecture and physical properties of cytoplasm: volume, viscosity, diffusion, intracellular surface area. Int Rev Cytol 192:189-221.

46. Fuller, B. G. 2010. Self-organization of intracellular gradients during mitosis. Cell Div 5:5.

47. Fulton, A. B. 1982. How crowded is the cytoplasm? Cell 30:345-347.

48. Ellis, R. J., and A. P. Minton. 2003. Cell biology: join the crowd. Nature 425:27-28.

49. Zimmerman, S. B., and S. O. Trach. 1991. Estimation of macromolecule concentrations and excluded volume effects for the cytoplasm of Escherichia coli. Journal of Molecular Biology 222:599-620.

50. Lanni F, W. A., Taylor DL. 1985. Structural organization of interphase 3T3 fibroblasts studied by total internal reflection fluorescence microscopy. Journal of Cell Biology 100:1091-1102.

51. Luby-Phelps, K. 2013. The physical chemistry of cytoplasm and its influence on cell function: an update. Mol Biol Cell 24:2593-2596.

52. de Heredia, M. L., and R.-P. Jansen. 2004. mRNA localization and the cytoskeleton. Current Opinion in Cell Biology 16:80-85.

53. Holthuis Joost, C. M., and C. Ungermann. 2013. Cellular microcompartments constitute general suborganellar functional units in cells. In Biological Chemistry. 151.

54. Kuhn, W. 1934. Über die Gestalt fadenförmiger Moleküle in Lösungen. Kolloid-Zeitschrift 68:2-15.

55. Wedler, G. 2004. Lehrbuch der Physikalischen Chemie, 5. edition. Wiley-VCH Verlag GmbH & Co. KGaA, Darmstadt.

56. Minton, A. P. 1998. Molecular crowding: analysis of effects of high concentrations of inert cosolutes on biochemical equilibria and rates in terms of volume exclusion. Methods Enzymol 295:127-149.

57. McMillan, W. G., and J. E. Mayer. 1945. The Statistical Thermodynamics of Multicomponent Systems. J Chem Phys 13:276-305.

58. Reiss, H., H. L. Frisch, and J. L. Lebowitz. 1959. Statistical Mechanics of Rigid Spheres. The Journal of Chemical Physics 31:369-380.

59. Boublik, T. 1974. Statistical thermodynamics of convex molecule fluids. Mol Phys 27:1415-1427.

60. Gibbons, R. M. 1969. The scaled particle theory for particles of arbitrary shape. Molecular Physics 17:81-86.

61. Ogston, A. G., and P. Silpananta. 1970. The thermodynamics of interaction between Sephadex and penetrating solutes. Biochem J 116:171-175.

62. Ogston, A. G. 1970. On the interaction of solute molecules with porous networks. J Phys Chem 74:668-669.

63. Ogston, A. G. 1958. The spaces in a uniform random suspension of fibres. Transactions of the Faraday Society 54:1754-1757.

64. Ogston A.G., P. C. F. 1960. The Partition of Solutes between Buffer Solutions and Solutions Containing Hyaluronic Acid. Biochemical Journal 78:827-833.

65. Ross, P. D., and A. P. Minton. 1977. Analysis of non-ideal behavior in concentrated hemoglobin solutions. J Mol Biol 112:437-452.

66. Ross, P. D., and A. P. Minton. 1979. The effect of non-aggregating proteins upon the gelation of sickle cell hemoglobin: Model calculations and data analysis. Biochemical and Biophysical Research Communications 88:1308-1314.

67. Guttman, H. J., C. F. Anderson, and M. T. Record Jr. 1995. Analyses of thermodynamic data for concentrated hemoglobin solutions using scaled particle theory: implications for a simple two-state model of water in thermodynamic analyses of crowding in vitro and in vivo. Biophysical Journal 68:835-846.

68. Minton, A. P. 1983. The effect of volume occupancy upon the thermodynamic activity of proteins: some biochemical consequences. Mol Cell Biochem 55:119-140.

69. Zhou, H.-X. 2008. Protein folding in confined and crowded environments. Archives of Biochemistry and Biophysics 469:76-82.

70. Minton, A. P. 2005. Models for excluded volume interaction between an unfolded protein and rigid macromolecular cosolutes: macromolecular crowding and protein stability revisited. Biophys J 88:971-985.

71. Minton, A. P. 2013. Quantitative assessment of the relative contributions of steric repulsion and chemical interactions to macromolecular crowding. Biopolymers 99:239-244.

72. Zhou, H. X. 2013. Influence of crowded cellular environments on protein folding, binding, and oligomerization: biological consequences and potentials of atomistic modeling. FEBS Lett 587:1053-1061.

73. Bloustine, J., T. Virmani, G. M. Thurston, and S. Fraden. 2006. Light Scattering and Phase Behavior of Lysozyme-Poly(Ethylene Glycol) Mixtures. Physical Review Letters 96:087803.

74. Tubio, G., B. Nerli, and G. Picó. 2004. Relationship between the protein surface hydrophobicity and its partitioning behaviour in aqueous two-phase systems of polyethyleneglycol–dextran. Journal of Chromatography B 799:293-301.

75. Winzor, D. J., and P. R. Wills. 2006. Molecular crowding effects of linear polymers in protein solutions. Biophysical Chemistry 119:186-195.

76. Miklos, A. C., M. Sarkar, Y. Wang, and G. J. Pielak. 2011. Protein Crowding Tunes Protein Stability. Journal of the American Chemical Society 133:7116-7120.

77. Armstrong, J. K., R. B. Wenby, H. J. Meiselman, and T. C. Fisher. 2004. The hydrodynamic radii of macromolecules and their effect on red blood cell aggregation. Biophys J 87:4259-4270.

78. Stagg, L., S. Q. Zhang, M. S. Cheung, and P. Wittung-Stafshede. 2007. Molecular crowding enhances native structure and stability of alpha/beta protein flavodoxin. Proc Natl Acad Sci U S A 104:18976-18981.

79. Homouz, D., L. Stagg, P. Wittung-Stafshede, and M. S. Cheung. 2009. Macromolecular Crowding Modulates Folding Mechanism of α/β Protein Apoflavodoxin. Biophysical Journal 96:671-680.

80. Homouz, D., H. Sanabria, M. N. Waxham, and M. S. Cheung. 2009. Modulation of Calmodulin Plasticity by the Effect of Macromolecular Crowding. Journal of Molecular Biology 391:933-943.

81. Bohrer, M. P., G. D. Patterson, and P. J. Carroll. 1984. Hindered diffusion of dextran and ficoll in microporous membranes. Macromolecules 17:1170-1173.

82. Venturoli, D., and B. Rippe. 2005. Ficoll and dextran vs. globular proteins as probes for testing glomerular permselectivity: effects of molecular size, shape, charge, and deformability. Am J Physiol Renal Physiol 288:F605-613.

83. Fodeke, A. A., and A. P. Minton. 2010. Quantitative characterization of polymer-polymer, protein-protein, and polymer-protein interaction via tracer sedimentation equilibrium. J Phys Chem B 114:10876-10880.

84. Davidson, M. G., and W. M. Deen. 1988. Hindered diffusion of water-soluble macromolecules in membranes. Macromolecules 21:3474-3481.

85. Granath, K. A. 1958. Solution properties of branched dextrans. Journal of Colloid Science 13:308-328.

86. del Álamo, M., G. Rivas, and M. G. Mateu. 2005. Effect of Macromolecular Crowding Agents on Human Immunodeficiency Virus Type 1 Capsid Protein Assembly In Vitro. Journal of Virology 79:14271-14281.

87. Fu, C.-y., M. C. Morais, A. J. Battisti, M. G. Rossmann, and P. E. Prevelige Jr. 2007. Molecular Dissection of Ø29 Scaffolding Protein Function in an in Vitro Assembly System. Journal of Molecular Biology 366:1161-1173.

88. Snoussi, K., and B. Halle. 2005. Protein Self-Association Induced by Macromolecular Crowding: A Quantitative Analysis by Magnetic Relaxation Dispersion. Biophysical Journal 88:2855-2866.

89. Díaz-López, T., C. Dávila-Fajardo, F. Blaesing, M. P. Lillo, and R. Giraldo. 2006. Early Events in the Binding of the pPS10 Replication Protein RepA to Single Iteron and Operator DNA Sequences. Journal of Molecular Biology 364:909-920.

90. Zorrilla, S., G. Rivas, A. U. Acuña, and M. P. Lillo. 2004. Protein self-association in crowded protein solutions: A time-resolved fluorescence polarization study. Protein Science 13:2960-2969.

91. Aguilar, X., C. F. Weise, T. Sparrman, M. Wolf-Watz, and P. Wittung-Stafshede. 2011. Macromolecular Crowding Extended to a Heptameric System: The Co-chaperonin Protein 10. Biochemistry 50:3034-3044.

92. Jiao, M., H.-T. Li, J. Chen, A. P. Minton, and Y. Liang. 2010. Attractive Protein-Polymer Interactions Markedly Alter the Effect of Macromolecular Crowding on Protein Association Equilibria. Biophysical Journal 99:914-923.

93. Zhou, H. X., G. Rivas, and A. P. Minton. 2008. Macromolecular crowding and confinement: biochemical, biophysical, and potential physiological consequences. Annu Rev Biophys 37:375-397.

94. Homchaudhuri, L., N. Sarma, and R. Swaminathan. 2006. Effect of crowding by dextrans and Ficolls on the rate of alkaline phosphatase–catalyzed hydrolysis: A size-dependent investigation. Biopolymers 83:477-486.

95. Morán-Zorzano, M. T., A. M. Viale, F. J. Muñoz, N. Alonso-Casajús, G. G. Eydallín, B. Zugasti, E. Baroja-Fernández, and J. Pozueta-Romero. 2007. Escherichia coli AspP activity is enhanced by macromolecular crowding and by both glucose-1,6-bisphosphate and nucleotide-sugars. FEBS Letters 581:1035-1040.

96. Derham, B. K., and J. J. Harding. 2006. The effect of the presence of globular proteins and elongated polymers on enzyme activity. Biochimica et Biophysica Acta (BBA) - Proteins and Proteomics 1764:1000-1006.

97. Pozdnyakova, I., and P. Wittung-Stafshede. 2010. Non-linear effects of macromolecular crowding on enzymatic activity of multi-copper oxidase. Biochimica et Biophysica Acta (BBA) - Proteins and Proteomics 1804:740-744.

98. Vöpel, T., and G. I. Makhatadze. 2012. Enzyme activity in the crowded milieu. PLoS One 7:e39418.

99. Ittah, V., E. Kahana, D. Amir, and E. Haas. 2004. Applications of time-resolved resonance energy transfer measurements in studies of the molecular crowding effect. Journal of Molecular Recognition 17:448-455.

100. Hong, J., and L. M. Gierasch. 2010. Macromolecular crowding remodels the energy landscape of a protein by favoring a more compact unfolded state. J Am Chem Soc 132:10445-10452.

101. Mikaelsson, T., J. Ådén, Lennart B. Å. Johansson, and P. Wittung-Stafshede. 2013. Direct Observation of Protein Unfolded State Compaction in the Presence of Macromolecular Crowding. Biophysical Journal 104:694-704.

102. Perham, M., L. Stagg, and P. Wittung-Stafshede. 2007. Macromolecular crowding increases structural content of folded proteins. FEBS Letters 581:5065-5069.

103. Dhar, A., A. Samiotakis, S. Ebbinghaus, L. Nienhaus, D. Homouz, M. Gruebele, and M. S. Cheung. 2010. Structure, function, and folding of phosphoglycerate kinase are strongly perturbed by macromolecular crowding. Proc Natl Acad Sci U S A 107:17586-17591.

104. McPhie, P., Y.-s. Ni, and A. P. Minton. 2006. Macromolecular Crowding Stabilizes the Molten Globule Form of Apomyoglobin with Respect to Both Cold and Heat Unfolding. Journal of Molecular Biology 361:7-10.

105. Sasaki, Y., D. Miyoshi, and N. Sugimoto. 2007. Regulation of DNA nucleases by molecular crowding. Nucleic Acids Research 35:4086-4093.

106. Kulothungan, S. R., M. Das, M. Johnson, C. Ganesh, and R. Varadarajan. 2009. Effect of Crowding Agents, Signal Peptide, and Chaperone SecB on the Folding and Aggregation of E. coli Maltose Binding Protein. Langmuir 25:6637-6648.

107. Monterroso, B., and A. P. Minton. 2007. Effect of high concentration of inert cosolutes on the refolding of an enzyme: carbonic anhydrase B in sucrose and ficoll 70. J Biol Chem 282:33452-33458.

108. van den Berg, B., R. Wain, C. M. Dobson, and R. J. Ellis. 2000. Macromolecular crowding perturbs protein refolding kinetics: implications for folding inside the cell. EMBO J 19:3870-3875.

109. van den Berg, B., R. J. Ellis, and C. M. Dobson. 1999. Effects of macromolecular crowding on protein folding and aggregation. EMBO J 18:6927-6933.

110. Homouz, D., M. Perham, A. Samiotakis, M. S. Cheung, and P. Wittung-Stafshede. 2008. Crowded, cell-like environment induces shape changes in aspherical protein. Proceedings of the National Academy of Sciences 105:11754-11759.

111. Stagg, L., A. Christiansen, and P. Wittung-Stafshede. 2010. Macromolecular Crowding Tunes Folding Landscape of Parallel α/β Protein, Apoflavodoxin. Journal of the American Chemical Society 133:646-648.

112. Ai, X., Z. Zhou, Y. Bai, and W.-Y. Choy. 2006. 15N NMR Spin Relaxation Dispersion Study of the Molecular Crowding Effects on Protein Folding under Native Conditions. Journal of the American Chemical Society 128:3916-3917.

113. Qin, S., and H.-X. Zhou. 2009. Atomistic Modeling of Macromolecular Crowding Predicts Modest Increases in Protein Folding and Binding Stability. Biophysical Journal 97:12-19.

114. Sanbo Qin and Lu Cai and Huan-Xiang, Z. 2012. A method for computing association rate constants of atomistically represented proteins under macromolecular crowding. Physical Biology 9:066008.

115. Sanbo Qin and Jeetain Mittal and Huan-Xiang, Z. 2013. Folding free energy surfaces of three small proteins under crowding: validation of the postprocessing method by direct simulation. Physical Biology 10:045001.

116. Cheung, J. K., and T. M. Truskett. 2005. Coarse-Grained Strategy for Modeling Protein Stability in Concentrated Solutions. Biophysical Journal 89:2372-2384.

117. Cheung, M. S., and D. Thirumalai. 2007. Effects of Crowding and Confinement on the Structures of the Transition State Ensemble in Proteins. The Journal of Physical Chemistry B 111:8250-8257.

118. Mittal, J., and R. B. Best. 2010. Dependence of Protein Folding Stability and Dynamics on the Density and Composition of Macromolecular Crowders. Biophysical Journal 98:315-320.

119. Batra, J., K. Xu, S. Qin, and H.-X. Zhou. 2009. Effect of Macromolecular Crowding on Protein Binding Stability: Modest Stabilization and Significant Biological Consequences. Biophysical Journal 97:906-911.

120. Tsao, D., and N. V. Dokholyan. 2010. Macromolecular crowding induces polypeptide compaction and decreases folding cooperativity. Phys Chem Chem Phys 12:3491-3500.

121. Goldenberg, D. P. 2003. Computational simulation of the statistical properties of unfolded proteins. J Mol Biol 326:1615-1633.

122. McGuffee, S. R., and A. H. Elcock. 2010. Diffusion, Crowding & Protein Stability in a Dynamic Molecular Model of the Bacterial Cytoplasm. PLoS Comput Biol 6:e1000694.

123. Wang, Q., and Margaret S. Cheung. 2012. A Physics-Based Approach of Coarse-Graining the Cytoplasm of Escherichia coli (CGCYTO). Biophysical Journal 102:2353-2361.

124. Pace, C. N., and K. L. Shaw. 2000. Linear extrapolation method of analyzing solvent denaturation curves. Proteins Suppl 4:1-7.

125. Pace, C. N. 1986. Determination and analysis of urea and guanidine hydrochloride denaturation curves. Methods Enzymol 131:266-280.

126. Scholtz, J. M., G. R. Grimsley, and C. N. Pace. 2009. Solvent denaturation of proteins and interpretations of the m value. Methods Enzymol 466:549-565.

127. Myers, J. K., C. Nick Pace, and J. Martin Scholtz. 1995. Denaturant m values and heat capacity changes: Relation to changes in accessible surface areas of protein unfolding. Protein Science 4:2138-2148.

128. Meuzelaar, H., K. A. Marino, A. Huerta-Viga, M. R. Panman, L. E. J. Smeenk, A. J. Kettelarij, J. H. van Maarseveen, P. Timmerman, P. G. Bolhuis, and S. Woutersen. 2013. Folding Dynamics of the Trp-Cage Miniprotein: Evidence for a Native-Like Intermediate from Combined Time-Resolved Vibrational Spectroscopy and Molecular Dynamics Simulations. The Journal of Physical Chemistry B 117:11490-11501.

129. Prigozhin, M. B., Y. Liu, A. J. Wirth, S. Kapoor, R. Winter, K. Schulten, and M. Gruebele. 2013. Misplaced helix slows down ultrafast pressure-jump protein folding. Proceedings of the National Academy of Sciences 110:8087-8092.

130. Chance, B. 1940. The accelerated flow method for rapid reactions. Journal of the Franklin Institute 229:737-766.

131. Tanford, C. 1970. Protein denaturation. C. Theoretical models for the mechanism of denaturation. Adv Protein Chem 24:1-95.

132. Jackson, S. E. 1998. How do small single-domain proteins fold? Fold Des 3:R81-91.

133. Oliveberg, M., Y. J. Tan, M. Silow, and A. R. Fersht. 1998. The changing nature of the protein folding transition state: implications

for the shape of the free-energy profile for folding. J Mol Biol 277:933-943.

134. Brandts, J. F., H. R. Halvorson, and M. Brennan. 1975. Consideration of the Possibility that the slow step in protein denaturation reactions is due to cis-trans isomerism of proline residues. Biochemistry 14:4953-4963.

135. Schmid, F. X., and R. L. Baldwin. 1978. Acid catalysis of the formation of the slow-folding species of RNase A: evidence that the reaction is proline isomerization. Proc Natl Acad Sci U S A 75:4764-4768.

136. Schmid, F. X., R. Grafl, A. Wrba, and J. J. Beintema. 1986. Role of proline peptide bond isomerization in unfolding and refolding of ribonuclease. Proc Natl Acad Sci U S A 83:872-876.

137. Wilson, C. J., and P. Wittung-Stafshede. 2005. Snapshots of a Dynamic Folding Nucleus in Zinc-Substituted Pseudomonas aeruginosa Azurin. Biochemistry 44:10054-10062.

138. Ternström, T., U. Mayor, M. Akke, and M. Oliveberg. 1999. From snapshot to movie: φ analysis of protein folding transition states taken one step further. Proceedings of the National Academy of Sciences 96:14854-14859.

139. Sánchez, I. E., and T. Kiefhaber. 2003. Origin of Unusual φ-values in Protein Folding: Evidence Against Specific Nucleation Sites. Journal of Molecular Biology 334:1077-1085.

140. Sánchez, I. E., and T. Kiefhaber. 2003. Evidence for Sequential Barriers and Obligatory Intermediates in Apparent Two-state Protein Folding. Journal of Molecular Biology 325:367-376.

141. Naganathan, A. N., and V. Muñoz. 2010. Insights into protein folding mechanisms from large scale analysis of mutational effects. Proceedings of the National Academy of Sciences 107:8611-8616.

142. Capaldi, A. P., C. Kleanthous, and S. E. Radford. 2002. Im7 folding mechanism: misfolding on a path to the native state. Nat Struct Biol 9:209-216.

143. Chiti, F., N. Taddei, P. M. White, M. Bucciantini, F. Magherini, M. Stefani, and C. M. Dobson. 1999. Mutational analysis of acylphosphatase suggests the importance of topology and contact order in protein folding. Nat Struct Biol 6:1005-1009.

144. Grantcharova, V. P., D. S. Riddle, J. V. Santiago, and D. Baker. 1998. Important role of hydrogen bonds in the structurally polarized

transition state for folding of the src SH3 domain. Nat Struct Biol 5:714-720.

145. Jackson, S. E., N. elMasry, and A. R. Fersht. 1993. Structure of the hydrophobic core in the transition state for folding of chymotrypsin inhibitor 2: a critical test of the protein engineering method of analysis. Biochemistry 32:11270-11278.

146. Miller, G. L. 1959. Use of Dinitrosalicylic Acid Reagent for Determination of Reducing Sugar. Analytical Chemistry 31:426-428.

147. Adman, E. T. 1991. Copper protein structures. Adv Protein Chem 42:145-197.

148. Engman, K. C., A. Sandberg, J. Leckner, and B. G. Karlsson. 2004. Probing the influence on folding behavior of structurally conserved core residues in P. aeruginosa apo-azurin. Protein Sci 13:2706-2715.

149. Wilson, C. J., D. Apiyo, and P. Wittung-Stafshede. 2006. Solvation of the folding-transition state in Pseudomonas aeruginosa azurin is modulated by metal: Solvation of azurin's folding nucleus. Protein Sci 15:843-852.

150. Pozdnyakova, I., J. Guidry, and P. Wittung-Stafshede. 2002. Studies of Pseudomonas aeruginosa azurin mutants: cavities in beta-barrel do not affect refolding speed. Biophysical Journal 82:2645-2651.

151. Pozdnyakova, I., and P. Wittung-Stafshede. 2003. Approaching the speed limit for Greek Key beta-barrel formation: transition-state movement tunes folding rate of zinc-substituted azurin. Biochim Biophys Acta 1651:1-4.

152. Pozdnyakova, I., and P. Wittung-Stafshede. 2002. If space is provided, bulky modification on the rim of azurin's beta-barrel results in folded protein. FEBS Lett 531:209-214.

153. Neupert, W. 1997. Protein Import into Mitochondria. Annual Review of Biochemistry 66:863-917.

154. Kadenbach, B. 1992. Book Review: Cytochromes C. Evolutionary, Structural and Physicochemical Aspects. (Springer Series in Molecular Biology). By G. R. Moore And G. W. Pettigrew. Angewandte Chemie International Edition in English 31:1098-1098.

155. Hamada, D., Y. Kuroda, M. Kataoka, S. Aimoto, T. Yoshimura, and Y. Goto. 1996. Role of heme axial ligands in the conformational stability of the native and molten globule states of horse cytochrome c. J Mol Biol 256:172-186.

156. Brems, D. N., and E. Stellwagen. 1983. Manipulation of the observed kinetic phases in the refolding of denatured ferricytochromes c. J Biol Chem 258:3655-3660.

157. Segel, D. J., A. L. Fink, K. O. Hodgson, and S. Doniach. 1998. Protein Denaturation: A Small-Angle X-ray Scattering Study of the Ensemble of Unfolded States of Cytochrome c. Biochemistry 37:12443-12451.

158. Tsong, T. Y. 1974. The Trp-59 fluorescence of ferricytochrome c as a sensitive measure of the over-all protein conformation. J Biol Chem 249:1988-1990.

159. Tsong, T. Y. 1975. An acid induced conformational transition of denatured cytochrome c in urea and guanidine hydrochloride solutions. Biochemistry 14:1542-1547.

160. Pascher, T., J. P. Chesick, J. R. Winkler, and H. B. Gray. 1996. Protein Folding Triggered by Electron Transfer. Science 271:1558-1560.

161. Goldbeck, R. A., Y. G. Thomas, E. Chen, R. M. Esquerra, and D. S. Kliger. 1999. Multiple pathways on a protein-folding energy landscape: Kinetic evidence. Proceedings of the National Academy of Sciences 96:2782-2787.

162. Goldbeck, R., E. Chen, and D. Kliger. 2009. Early Events, Kinetic Intermediates and the Mechanism of Protein Folding in Cytochrome c. International Journal of Molecular Sciences 10:1476-1499.

163. Chen, E., M. J. Wood, A. L. Fink, and D. S. Kliger. 1998. Time-Resolved Circular Dichroism Studies of Protein Folding Intermediates of Cytochrome c†. Biochemistry 37:5589-5598.

164. Muralidhara, B. K., and P. Wittung-Stafshede. 2004. Thermal Unfolding of Apo and Holo Desulfovibrio desulfuricans Flavodoxin: Cofactor Stabilizes Folded and Intermediate States†. Biochemistry 43:12855-12864.

165. Muralidhara, B. K., R. Rathinakumar, and P. Wittung-Stafshede. 2006. Folding of Desulfovibrio desulfuricans flavodoxin is accelerated by cofactor fly-casting. Archives of Biochemistry and Biophysics 451:51-58.

166. Caldeira, J., P. N. Palma, M. Regalla, J. Lampreia, J. Calvete, W. Schäfer, J. Legall, I. Moura, and J. J. Moura. 1994. Primary sequence, oxidation-reduction potentials and tertiary-structure prediction of Desulfovibrio desulfuricans ATCC 27774 flavodoxin. Eur J Biochem 220:987-995.

167. Apiyo, D., J. Guidry, and P. Wittung-Stafshede. 2000. No cofactor effect on equilibrium unfolding of Desulfovibrio desulfuricans flavodoxin. Biochim Biophys Acta 1479:214-224.

168. Muralidhara, B. K., and P. Wittung-Stafshede. 2004. Thermal unfolding of Apo and Holo Desulfovibrio desulfuricans flavodoxin: cofactor stabilizes folded and intermediate states. Biochemistry 43:12855-12864.

169. Stagg, L., A. Samiotakis, D. Homouz, M. S. Cheung, and P. Wittung-Stafshede. 2010. Residue-Specific Analysis of Frustration in the Folding Landscape of Repeat β/α Protein Apoflavodoxin. Journal of Molecular Biology 396:75-89.

170. Kihara, T. 1953. Virial Coefficients and Models of Molecules in Gases. Reviews of Modern Physics 25:831-843.

171. Zhou, H.-X. 2004. Protein folding and binding in confined spaces and in crowded solutions. Journal of Molecular Recognition 17:368-375.

172. Zhou, H.-X. 2002. Dimensions of Denatured Protein Chains from Hydrodynamic Data. The Journal of Physical Chemistry B 106:5769-5775.

173. Waegele, M. M., and F. Gai. 2011. Power-law dependence of the melting temperature of ubiquitin on the volume fraction of macromolecular crowders. The Journal of Chemical Physics 134:095104-095106.

174. Batra, J., K. Xu, and H. X. Zhou. 2009. Nonadditive effects of mixed crowding on protein stability. Proteins 77:133-138.

175. Laurent, T. C., and J. Killander. 1964. Theory of gel filtration and its experimental verification. Journal of Chromatography 14:317-330.

176. Sánchez, I. E., and T. Kiefhaber. 2003. Hammond Behavior versus Ground State Effects in Protein Folding: Evidence for Narrow Free Energy Barriers and Residual Structure in Unfolded States. Journal of Molecular Biology 327:867-884.

177. Dix, J. A., and A. S. Verkman. 2008. Crowding effects on diffusion in solutions and cells. Annu Rev Biophys 37:247-263.

178. Zeeb, M., M. H. Jacob, T. Schindler, and J. Balbach. 2003. 15N relaxation study of the cold shock protein CspB at various solvent viscosities. J Biomol NMR 27:221-234.

179. Li, C., Y. Wang, and G. J. Pielak. 2009. Translational and Rotational Diffusion of a Small Globular Protein under Crowded Conditions. The Journal of Physical Chemistry B 113:13390-13392.

180. Wang, Y., C. Li, and G. J. Pielak. 2010. Effects of proteins on protein diffusion. J Am Chem Soc 132:9392-9397.

181. Sasahara, K., P. McPhie, and A. P. Minton. 2003. Effect of dextran on protein stability and conformation attributed to macromolecular crowding. J Mol Biol 326:1227-1237.

182. Wang, Y., H. He, and S. Li. 2010. Effect of Ficoll 70 on thermal stability and structure of creatine kinase. Biochemistry (Mosc) 75:648-654.

183. Benton, L. A., A. E. Smith, G. B. Young, and G. J. Pielak. 2012. Unexpected effects of macromolecular crowding on protein stability. Biochemistry 51:9773-9775.

184. Wang, Y., M. Sarkar, A. E. Smith, A. S. Krois, and G. J. Pielak. 2012. Macromolecular Crowding and Protein Stability. Journal of the American Chemical Society 134:16614-16618.

185. Malik, A., J. Kundu, S. K. Mukherjee, and P. K. Chowdhury. 2012. Myoglobin Unfolding in Crowding and Confinement. The Journal of Physical Chemistry B 116:12895-12904.

186. Sotomayor-Pérez, A.-C., O. Subrini, A. Hessel, D. Ladant, and A. Chenal. 2013. Molecular Crowding Stabilizes Both the Intrinsically Disordered Calcium-Free State and the Folded Calcium-Bound State of a Repeat in Toxin (RTX) Protein. Journal of the American Chemical Society 135:11929-11934.

187. Liu, Z., W. Weng, R. M. Bookchin, V. L. Lew, and F. A. Ferrone. 2008. Free energy of sickle hemoglobin polymerization: a scaled-particle treatment for use with dextran as a crowding agent. Biophys J 94:3629-3634.

188. Spencer, D. S., K. Xu, T. M. Logan, and H. X. Zhou. 2005. Effects of pH, salt, and macromolecular crowding on the stability of FK506-binding protein: an integrated experimental and theoretical study. J Mol Biol 351:219-232.

189. Kuhnert, D. C., S. Gildenhuys, and H. W. Dirr. 2008. Effect of macromolecular crowding on the stability of monomeric glutaredoxin 2 and dimeric glutathione transferase A1-1. South African Journal of Science 104:76-80.

190. Segel, D. J., A. L. Fink, K. O. Hodgson, and S. Doniach. 1998. Protein denaturation: a small-angle X-ray scattering study of the ensemble of unfolded states of cytochrome c. Biochemistry 37:12443-12451.

191. Millet, I. S., L. E. Townsley, F. Chiti, S. Doniach, and K. W. Plaxco. 2001. Equilibrium Collapse and the Kinetic 'Foldability' of Proteins. Biochemistry 41:321-325.

192. Sarkar, M., C. Li, and G. Pielak. 2013. Soft interactions and crowding. Biophysical Reviews 5:187-194.

193. Fodeke, A. A., and A. P. Minton. 2011. Quantitative Characterization of Temperature-Independent and Temperature-Dependent Protein–Protein Interactions in Highly Nonideal Solutions. The Journal of Physical Chemistry B 115:11261-11268.

194. Brandt, T., J. L. Kaar, A. R. Fersht, and D. B. Veprintsev. 2012. Stability of p53 homologs. PLoS One 7:e47889.

195. Walkiewicz, K., A. S. Benitez Cardenas, C. Sun, C. Bacorn, G. Saxer, and Y. Shamoo. 2012. Small changes in enzyme function can lead to surprisingly large fitness effects during adaptive evolution of antibiotic resistance. Proc Natl Acad Sci U S A 109:21408-21413.

196. Metcalfe, J., D. Dhindsa, M. Edwards, and M. A. 1969. Decreased affinity of blood for oxygen in patients with low-output heart failure. Circ. Res. 25:47-51.

197. Minton, A. P., G. C. Colclasure, and J. C. Parker. 1992. Model for the role of macromolecular crowding in regulation of cellular volume. Proc Natl Acad Sci U S A 89:10504-10506.

198. Zhang, J. 2000. Protein-length distributions for the three domains of life. Trends in Genetics 16:107-109.

199. Dill, K. A., K. Ghosh, and J. D. Schmit. 2011. Physical limits of cells and proteomes. Proceedings of the National Academy of Sciences 108:17876-17882.

200. Gershenson, A., and L. M. Gierasch. 2011. Protein folding in the cell: challenges and progress. Current Opinion in Structural Biology 21:32-41.

201. Ghaemmaghami, S., and T. G. Oas. 2001. Quantitative protein stability measurement in vivo. Nat Struct Biol 8:879-882.

202. Ignatova, Z., and L. M. Gierasch. 2004. Monitoring protein stability and aggregation in vivo by real-time fluorescent labeling. Proceedings of the National Academy of Sciences of the United States of America 101:523-528.

203. Ignatova, Z., and L. Gierasch. 2009. A Method for Direct Measurement of Protein Stability In Vivo. In Protein Structure, Stability, and Interactions. J. W. Shriver, editor. Humana Press. 165-178.

204. Dhar, A., K. Girdhar, D. Singh, H. Gelman, S. Ebbinghaus, and M. Gruebele. 2011. Protein stability and folding kinetics in the nucleus and endoplasmic reticulum of eucaryotic cells. Biophys J 101:421-430.

205. Ito, Y., and P. Selenko. 2010. Cellular structural biology. Current Opinion in Structural Biology 20:640-648.

206. Pielak, G. J., C. Li, A. C. Miklos, A. P. Schlesinger, K. M. Slade, G.-F. Wang, and I. G. Zigoneanu. 2008. Protein Nuclear Magnetic Resonance under Physiological Conditions†. Biochemistry 48:226-234.

207. Sakakibara, D., A. Sasaki, T. Ikeya, J. Hamatsu, T. Hanashima, M. Mishima, M. Yoshimasu, N. Hayashi, T. Mikawa, M. Wälchli, B. O. Smith, M. Shirakawa, P. Güntert, and Y. Ito. 2009. Protein structure determination in living cells by in-cell NMR spectroscopy. Nature 458:102-105.

208. Dedmon, M. M., C. N. Patel, G. B. Young, and G. J. Pielak. 2002. FlgM gains structure in living cells. Proceedings of the National Academy of Sciences 99:12681-12684.

209. Bodart, J. F., J. M. Wieruszeski, L. Amniai, A. Leroy, I. Landrieu, A. Rousseau-Lescuyer, J. P. Vilain, and G. Lippens. 2008. NMR observation of Tau in Xenopus oocytes. J Magn Reson 192:252-257.

210. Inomata, K., A. Ohno, H. Tochio, S. Isogai, T. Tenno, I. Nakase, T. Takeuchi, S. Futaki, Y. Ito, H. Hiroaki, and M. Shirakawa. 2009. High-resolution multi-dimensional NMR spectroscopy of proteins in human cells. Nature 458:106-109.

211. Lippens, G., I. Landrieu, and X. Hanoulle. 2008. Studying posttranslational modifications by in-cell NMR. Chem Biol 15:311-312.

212. Selenko, P., D. P. Frueh, S. J. Elsaesser, W. Haas, S. P. Gygi, and G. Wagner. 2008. In situ observation of protein phosphorylation by high-resolution NMR spectroscopy. Nat Struct Mol Biol 15:321-329.

213. Jin, S., and A. S. Verkman. 2007. Single particle tracking of complex diffusion in membranes: simulation and detection of barrier, raft, and interaction phenomena. J Phys Chem B 111:3625-3632.

214. Seksek, O., J. Biwersi, and A. S. Verkman. 1997. Translational diffusion of macromolecule-sized solutes in cytoplasm and nucleus. J Cell Biol 138:131-142.

215. Swaminathan, R., C. P. Hoang, and A. S. Verkman. 1997. Photobleaching recovery and anisotropy decay of green fluorescent protein GFP-S65T in solution and cells: cytoplasmic viscosity probed by green fluorescent protein translational and rotational diffusion. Biophys J 72:1900-1907.

216. Weiss, M., M. Elsner, F. Kartberg, and T. Nilsson. 2004. Anomalous Subdiffusion Is a Measure for Cytoplasmic Crowding in Living Cells. Biophysical Journal 87:3518-3524.

217. Bacia, K., S. A. Kim, and P. Schwille. 2006. Fluorescence cross-correlation spectroscopy in living cells. Nat Methods 3:83-89.

218. Dauty, E., and A. S. Verkman. 2005. Actin cytoskeleton as the principal determinant of size-dependent DNA mobility in cytoplasm: a new barrier for non-viral gene delivery. J Biol Chem 280:7823-7828.

219. Dayel, M. J., E. F. Hom, and A. S. Verkman. 1999. Diffusion of green fluorescent protein in the aqueous-phase lumen of endoplasmic reticulum. Biophys J 76:2843-2851.

220. Verkman, A. S. 2002. Solute and macromolecule diffusion in cellular aqueous compartments. Trends in Biochemical Sciences 27:27-33.

221. Alexander Christiansen, Qian Wang, Margaret S. Cheung and Pernilla Wittung-Stafshede. 2013. Effects of macromolecular crowding agents on protein folding in vitro and in silico. Biophysical Reviews 5 (2), 137-145